EVALUATING HIMALAYAN TECTONIC MODELS

USING THE ALMORA-DADELDHURA KLIPPE

by

SOMIDDHO BOSU

DELORES M. ROBINSON, COMMITTEE CHAIR
IBRAHIM CEMEN
KIMBERLY GENAREAU
MARY DAVIS

A THESIS

Submitted in partial fulfilment of the requirements
for the degree of Master of Science
in the Department of Geological Sciences
in the Graduate School of
The University of Alabama

TUSCALOOSA, ALABAMA

2019

ABSTRACT

The Greater Himalayan klippen are erosionally isolated, thrust bounded rocks, overlying Lesser Himalayan rocks in the Himalayan thrust belt. Structural and thermochronological data gathered in the klippen illuminate how Greater Himalayan rocks were emplaced and deformed between ~30-10 Ma. The Almora-Dadeldhura klippe in northwest India and far western Nepal is composed of rocks with Greater and Tethyan Himalayan affinities. Researchers use interpretations of rock affinity, number of shear zones, metamorphic gradient, thermochronology and microstructural data to support the critical taper, channel flow, or wedge insertion models for the development of the Himalayan thrust belt. Channel flow is not supported if the timing of the Main Central Thrust (MCT) and South Tibet Detachment System (STDS) are interpreted to be different. Wedge insertion is not supported if the STDS in the hinterland and klippe are the same fault but do not slip at the same time. The critical taper model is the most difficult to refute because the model can accommodate slip in almost any part of a thrust belt as the thrust belt responds to maintain critical taper. The already published and original data, that support or refute each of the models are presented. A kinematic model is developed combining the existing thermochronology and structural data. In this model, the Almora-Dadeldhura klippe was emplaced over Lesser Himalayan rocks between 28-18 Ma if the klippe was formed by an intra-Greater Himalayan thrust or between 18-13 Ma if the fault that forms the klippe is the Main Central thrust. The building of the Lesser Himalayan duplex folded the overlying klippe rock to dip southward between ~10-4 Ma. The northern part of the klippe was folded to dip south,

beginning between 7-5 Ma due to the placement of the Main Boundary thrust and the Subhimalayan thrust system. This fits a model of forward propagating thrust system and conforms with the predictions of the critical taper model.

ACKNOWLEDGEMENTS

Research expenses were funded by The University of Alabama Graduate School, Graduate Students Association, Capstone International Center, and the Department of Geological Sciences, The University of Alabama. This research greatly benefited from discussions with Dr. Sean Long, Washington State University, Pullman, Mr. Arkajyoti Saha and Dr. Gautam Ghosh, Presidency University, Kolkata, India, Dr. Manish A. Mamtani and Dr. Renjith Ambady, Indian Institute of Technology, Kharagpur and Cam Hughes, University of Tennessee, Knoxville. I am indebted to my thesis committee and the committee chair for their invaluable inputs and guidance.

CONTENTS

LIST OF FIGURES

LIST OF TABLES

1. INTRODUCTION

Tectonic models developed for the Himalayan thrust belt are used to understand analogous orogens like the Sevier orogen in western North America (Hodges and Walker, 1992; Wells, 1997), Orocopia Mountains in western North America (Yin, 2002), Grenville orogen in eastern North America (Selleck et al., 2005; Jamieson et al., 2007; Rivers, 2008), Canadian Cordillera in western North America (DeCelles and Cavazza, 1999; Brown and Gibson, 2006; Kuiper et al., 2006), Caledonian orogen in Greenland (McClelland and Gilotti, 2003), Altai in central Asia, (Yang et al., 1992; Quand Zhang, 1994), Tanzania in Africa (Fritz et al., 2009), East African–Antarctic orogeny (Jacobs and Thomas, 2004), Petermann orogeny in Australia (Raimondo et al., 2009), and New England orogeny in Australia (Aitchison, 2010). The Himalayan thrust belt is also studied to understand climate-orogeny interaction (e.g., Copeland et al., 1987; Molnar and England 1990; Molnar et al., 1993; Kutzbach et al., 1993; Ramstein et al., 1997), and terrane accretion (e.g., Beck et al., 1995; Weller et al., 2015). Three competing tectonic models that illustrate the development of the Himalayan thrust belt include: 1) critical taper (e.g., Davis et al., 1983; Dahlen et al., 1984; Dahlen, 1990, Srivastava and Mitra, 1994; DeCelles et al., 2001; Robinson et al., 2006, Kohn, 2008); 2) channel flow (e.g., Grujic et al., 1996; Beaumont et al., 2001); and 3) wedge insertion (Yin, 2006; Webb et al., 2007; Webb et al., 2011). These models have different interpretations of how the metamorphic core, the Greater (or High) Himalayan rocks were emplaced, leading to different interpretations of the kinematic evolution of the Greater Himalayan klippen in the thrust belt.

The Greater Himalayan klippen are isolated folded thrust sheets composed of igneous and metamorphic rocks, overlying Lesser Himalayan rocks (Heim and Gansser, 1939; Valdiya, 1980; Srivastava and Mitra, 1996; Upreti and Le Fort, 1999; DeCelles et al., 2001; Gehrels et al., 2006; Mandal et al., 2014). The Almora-Dadeldhura klippe is the largest of these Greater Himalayan klippen, span from the Tons River in Garhwal in northwest India, to east of the Karnali River in far western Nepal (Figure 1). Because the klippe is ~350 km long, ~20-80 km wide and crosses into two countries, previous studies collected data from a limited region within the klippe (Valdiya, 1980; Stöcklin, 1980; Srivastava and Mitra, 1996; Valdiya and Kotlia, 2001; DeCelles et al., 2001; Robinson et al., 2006; Næraa et al., 2007; Joshi and Tiwari, 2009; Rawat and Sharma, 2011; Antolín et al., 2013; Mandal et al., 2014; Patel et al., 2015; He et al., 2016, LaRoche et al., 2016, van der Beek et al., 2016; Singh and Patel, 2017). Recent geochemical data from Kumaun (Mandal et al., 2014) and far western Nepal (Robinson et al., 2001; Gehrels et al., 2006) show that klippe rocks have detrital zircon age populations and εNd (epsilon-Neodymium) values similar to Greater and Tethyan Himalayan rocks, which are present north of the Main Central thrust (MCT). In India, the klippe appears to be composed entirely of Greater Himalayan rocks (Mandal et al., 2014), however, in Nepal, there are two isolated locations composed of Tethyan Himalayan rocks (Figure 1; Gehrels et al., 2006).

This study hypothesizes the Almora-Dadeldhura klippe as a Greater Himalayan thrust sheet and the shear zones in the klippe as intra-Greater Himalayan shear zones. According to this hypothesis, the intra-Greater Himalayan shear zones in the klippe were deformed during deformation towards the foreland. Because of spatial limitations of the collected data and tendency to support a particular idea, different models for the evolution of the Almora-Dadeldhura klippe have been developed. This paper will address 3 of the most prevalent models-

critical taper, channel flow and wedge insertion- to see how the available data matches their predictions. In this paper, I compile stratigraphic, metamorphic and thermochronologic data along with field observations and microstructure data from the Almora-Dadeldhura klippe and interpret the data in the context of the 3 competing models. Unintentional biases are revealed along with a discussion of the kinematic evolution of the Himalayan thrust belt.

2. REGIONAL GEOLOGY

The Himalayan thrust belt consists of deformed and metamorphosed sedimentary and igneous rocks (Heim and Gansser, 1939; Gansser, 1964; LeFort, 1975; Valdiya, 1980). The strata are folded and faulted across multiple, north dipping thrust faults (Figures 1 and 2).

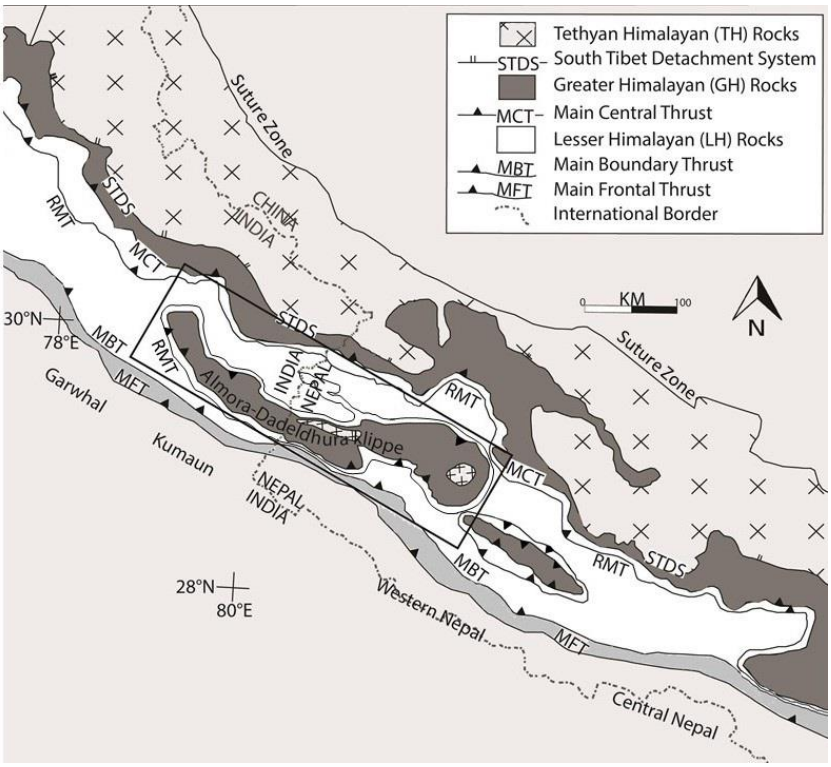

Figure 1. Simplified regional tectonostratigraphic map of the Himalayan thrust belt in Garwhal, Kumaun, and western and central Nepal. Modified after Robinson and Pearson (2013). Box with black outline shows location of Figure 4.

Major structures in the Himalayan thrust belt from north to south include the South Tibetan detachment system (STDS), Main Central thrust (MCT), Ramgarh-Munsiari thrust

(RMT), Lesser Himalayan duplex, Main Boundary thrust (MBT) and Main Frontal thrust (MFT). At depth, these surface faults connect with the Main Himalayan Thrust (MHT), which forms the basal décollement in the Himalayan thrust belt (e.g., Zhao et al., 1993). The Himalayan thrust belt spans from the Indus-Yarlung suture zone in the north and the Main Frontal thrust in the south. Tethyan Himalayan rocks are present between the suture zone and the STDS. Tethyan Himalayan rocks were deposited in Paleozoic-Mesozoic time as two passive margin sequences separated by a break up stage in Permian time (Garzanti, 1999). Deformation in the Tethyan Himalayan rocks occurred between the time India collided with Asia at ~58 Ma (e.g., DeCelles et al., 2014) to the time of intra-Greater Himalayan thrusting at ~28 Ma (Montomoli et al., 2013). The STDS was active between 25-23 Ma in western Nepal (Carosi et al., 2013). In Garhwal, ductile deformation on the STDS ceased by 15 Ma (Sen et al., 2015; Iaccarino et al., 2017; Montemagni et al., 2018); 50 km to the west, Searle et al. (1999) report an age of 23 Ma for the STDS. Although Tethyan Himalayan rocks can be metamorphosed to staurolite zone (Garhwal, Searle et al., 1993), these metamorphic rocks are present near the STDS, while most of the remaining Tethyan Himalayan section is unmetamorphosed sedimentary rocks (Hughes and Droser, 1992). In the Almora-Dadeldhura klippe, east of the Karnali River, the Tethyan Himalayan rocks are alternating biotite-muscovite schist with calcareous schist (Arita et al., 1984); however, along the Dadeldhura road, the rocks are phyllite, black slate and sandstone (Gehrels et al., 2006).

Greater Himalayan rocks exposed between the STDS and MCT are paragneiss, schist, calcsilicate and Cambrian-Ordovician orthogneiss, which are all intruded by Miocene leucogranite (Valdiya, 1980; Parrish and Hodges, 1996; Hodges, 2000; Robinson et al., 2001; Célérier et al., 2009). In Garhwal, the MCT may be active from 16-9 Ma (Montemagni et al.,

2018). In far western Nepal, the MCT may be active from 25-21 Ma, (DeCelles et al., 2001; Robinson et al., 2006). However, just east of the Almora-Dadeldhura klippe, Montomoli et al. (2013) state that the Main Central Thrust (MCT) was active between 18-13 Ma along the Karnali River. Along the Karnali River, the metamorphic temperatures in Greater Himalayan rocks range between 580-720 ºC and the pressures are 8-11 kbar, both decreasing up section (Yakimchuk and Godin, 2012). Rocks with Greater Himalayan affinities are also exposed in isolated klippen south of the MCT, and are described in chapter 4.

After motion on the MCT, deformation propagated southward into Lesser Himalayan rocks, forming the Ramgarh-Munsiari thrust somewhere between 17-7 Ma from a very poorly formed Ar age spectra (Robinson et al., 2006) and 20-16 Ma using forward modeling (Robinson and McQuarrie, 2012) in far western Nepal. East of the Almora-Dadeldhura klippe, Montomoli et al. (2013) has a youngest MCT age of 13 Ma. Thus, the Ramgarh-Munsiari thrust initiated after 13 Ma and then formed the Lesser Himalayan duplex, with the MBT as the last thrust sheet in the Lesser Himalayan duplex. In far western Nepal, the Lesser Himalayan duplex formed between 16-5 Ma (Robinson and McQuarrie 2012). First motion on the MBT is at ~4 Ma in central Nepal (Rösler et al., 1997; Ojha et al., 20098) but no ages are available from far western Nepal or Kumaun.

In Nepal, Lesser Himalayan rocks range from Paleoproterozoic and Mesoproterozoic to Tertiary in age (see Martin, 2017 for review), and are composed of quartzite, schist, orthogneiss, phyllite, carbonate rock, shale and lithic sandstone. In Kumaon, Lesser Himalayan rocks are Paleoproterozoic and Neoproterozoic in age (Mandel et al., 2014). In far western Nepal, Lesser Himalayan rocks are ~8.7-11 km thick (Robinson et al., 2006 and references therein), and 11 km thick in Kumaun (Srivasatava and Mitra, 1994; Célérier et al., 2009). Paleoproterozoic Lesser

Himalayan rocks are folded underneath Greater Himalayan rocks of the Almora-Dadeldhura klippe, and are carried by the Ramgarh-Munsiari thrust sheet (Robinson et al., 2006; Mandal et al., 2014).

Subhimalayan rocks are present between the MBT and MFT, south of the Almora-Dadeldhura klippe. Subhimalayan rocks consist of shallow-marine strata and continental deposits (e.g., Powers et al., 1998) and include the Siwalik Group. In Kumaon, the Lugad Gad Formation and Subathu Formation are present between the MBT and MFT. The Neogene Siwalik Group is an upward coarsening, fluvial siltstone and sandstone (e.g., DeCelles et al., 1998). The Lugad Gad Formation is a pale green, biotite-rich sandstone (Rupke, 1974), which is equivalent to the Early Miocene Dumri Formation of western Nepal and Kasauli/upper Dharamshala Formation of Himachal Pradesh (DeCelles et al., 1998; Najman, 2006). The Subathu Formation is Eocene in age, and contains marine to continental transition sequence (Bera et al., 2008). In Nepal, the foreland basin rocks, Dumri and Bhainskati Formations are only found north of the MBT. Thus, in Nepal, these rocks are included in the upper part of the Lesser Himalayan stratigraphy.

3. TECTONIC MODELS OF THE HIMALAYAN THRUST BELT

The critical taper model is one where the wedge deforms until a critical taper is attained, and a steady state is attained by continuous and simultaneous erosion and accretion of a critically tapered wedge (Davis et al., 1983; Dahlen, 1984). A wedge is formed by the basal dècollement and the topographic surface, with the angle of the wedge referred to as the critical taper (Dahlen, 1984). The critical taper model has been successfully applied in the Himalaya thrust belt (e.g., Srivastava and Mitra, 1994; DeCelles et al., 1998, 2001; Pearson, 2002; Robinson et al., 2006; Kohn, 2008; Long et al., 2011; Khanal and Robinson, 2013; Robinson and Martin, 2014; Bhattacharyya et al., 2015). The critical taper model predicts: (1) deformation propagated from

the hinterland towards the foreland with out-of-sequence faulting with <10 km of motion as the wedge tries to maintain the critical taper angle; (2) deformation under pure shear conditions (e.g., Long et al., 2016); (3) Tethyan Himalayan rock in the klippe is not bounded at the base by the STDS but it is possible that the contact is another fault or unconformity (e.g., Robinson et al., 2006).

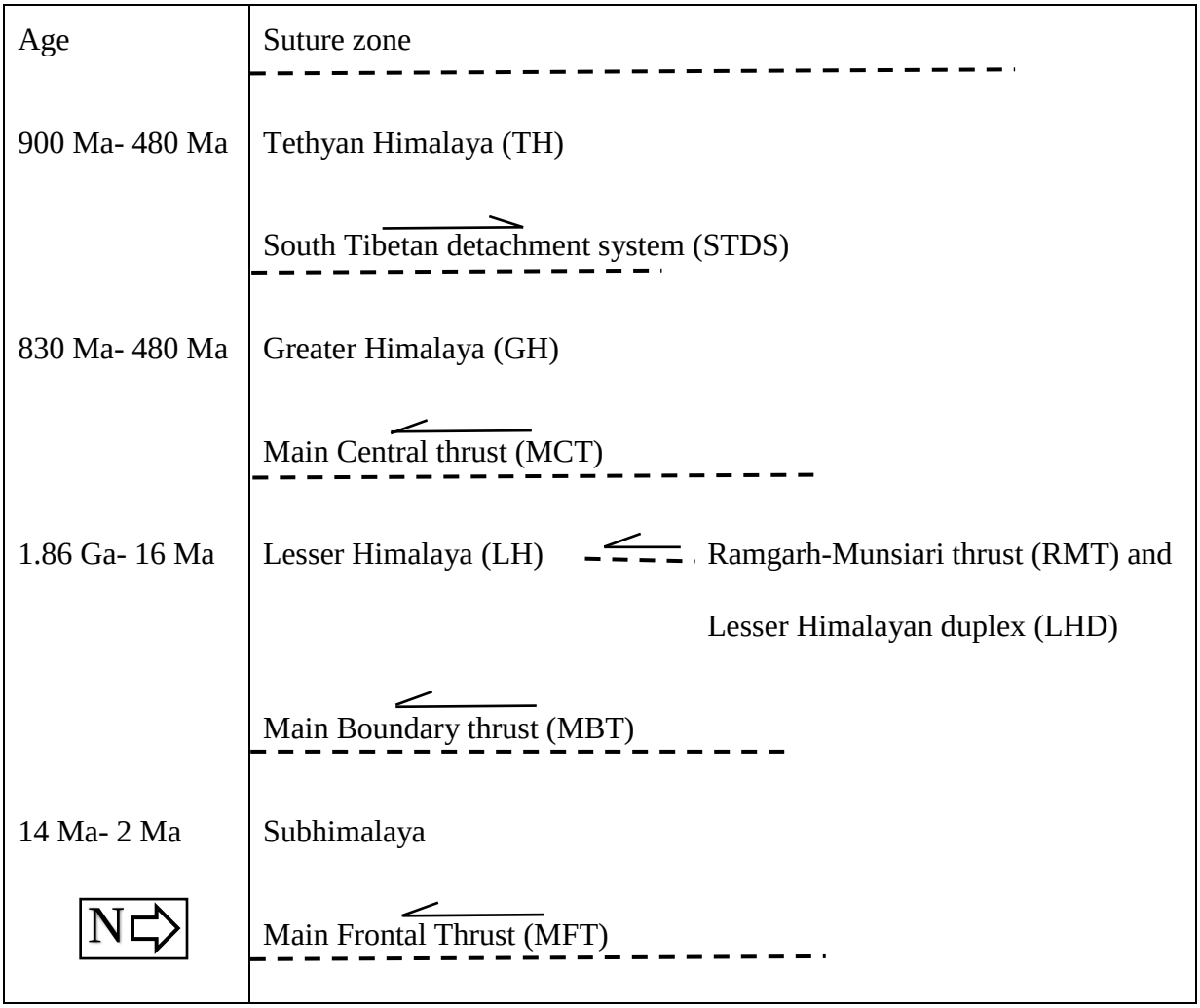

Figure 2. General tectonostratigraphic divisions, with the faults and the sense of motion (to the left- thrust; to the right- normal). The age of the corresponding stratigraphic unit is in the first column. Compiled and modified from Kashmir and Himachal Himalaya (Valdiya, 1980); Nepal Himalaya (Robinson et al., 2006); Kumaun Himalaya (Mandal et al., 2014). Ages of stratigraphic units are from western Nepal (DeCelles et al., 2001). See text for discussion of Lesser Himalayan rock ages.

Balanced cross sections in the far western Nepal treat Greater Himalayan rocks as a large slab of metamorphic material, and transports the rock southward along the MCT (e.g., DeCelles et al., 2001; Robinson et al., 2006). In the critical taper model, it does not matter if the Greater Himalayan rocks were emplaced on one sheet or multiple sheets over the Lesser Himalayan rocks. Also in the critical taper model, it does not matter whether the STDS is contemporaneous with the MCT or not.

Because of the large amount of melt found in Bhutan in Greater Himalayan rocks, Grujic et al. (1996) introduced the channel flow model, which was supported by the geophysical models of Nelson et al. (1996) and Hauck et al. (1998). Channel flow is a ductile extrusion model that advocates moving Greater Himalayan rocks to the surface between the MCT and STDS (Figure 3B); thus, these faults must be active at the same time with similar amounts of offset. The MCT and STDS are subparallel, and extend beneath the Tibetan Plateau, forming a partially molten ductile channel that exhumes Greater Himalayan rocks towards south (Nelson et al., 1996; Beaumont et al., 2001). Extrusion is enhanced by focused erosion where Greater Himalayan rocks come to the surface in the Himalayan thrust belt (Nelson et al., 1996). The origin of this middle-lower crust is Asian crust in Nelson et al. (1996), and from subducting Indian crust in Beaumont et al. (2001). The channel flow model predicts (Godin et al., 2006): (1) extrusion of the ductile channel remained continuous once initiated, with coeval shearing in the basal and roof thrusts; extrusion of the ductile Greater Himalayan rock is out-of-sequence (2) the metamorphic core deforms in co-axial flow with increasing simple shear component towards the roof thrust, (3) inverted metamorphic grade towards the top of the channel. If the STDS is not present in the klippe, it does not mean that channel flow did not occur, just that it is restricted to north of the MCT (see Robinson and Pearson, 2013).

Webb et al. (2007) advocates for the wedge insertion model (Yin, 2006), citing merging of the MCT with STDS towards the south in northwest India (Webb et al., 2011) and western Nepal (He et al., 2016). In the wedge insertion model, the STDS is a passive roof thrust where this roof thrust experienced shearing due to the insertion of Greater Himalayan rocks along the MCT between the Tethyan and Lesser Himalayan rocks like a wedge that tapers towards the foreland (Figure 3C). Depending on the relative direction of motion of the Greater Himalayan rocks and the hanging wall block, the STDS is predicted to have either top-north or top-south sense of shear (e.g., NW India, Patel et al., 1993; Figure 4 in Webb et al., 2007). The predictions of this model are as follows (Yin, 2006; Webb et al., 2007; Webb et al., 2011; He et al., 2016): (1) emplacement of the Greater Himalayan rocks is not facilitated by erosion; (2) a foreland-ward tapering wedge will merge the MCT and STDS at the tip of the Greater Himalayan rocks. At this tip, the merged fault will place Tethyan Himalayan rocks over Lesser Himalayan rocks; (3) south of the tapering wedge tip, the merged fault will have top-south shear; north of the tip, the STDS will have top-north shear and MCT will have top-south shear (see Figure 13 in He et al., 2016).

The predicted differences in the tectonic architecture and stratigraphy of the thrust belt makes the Almora-Dadeldhura klippe the ideal place to determine which of these tectonic models are most appropriate (Figure 3). The critical taper model predicts that the Tethyan Himalayan/Greater Himalayan contact in the klippen is not the STDS; however, it could be another fault or a stratigraphic contact (Gehrels et al., 2006; Figure 3A). The channel flow model predicts that MCT and STDS are parallel in the klippe, with Greater Himalayan rocks carried by the MCT and Tethyan Himalayan rocks in the STDS hanging wall (Antolín et al., 2013; La Roche et al., 2016; Figure 3B). The wedge insertion model predicts a merging of MCT and

STDS under the klippe with the entire klippe containing Tethyan Himalayan rocks and a tapering wedge of Greater Himalayan rocks between the converging MCT and STDS north of the klippe (He et al., 2016; Figure 3C). In the critical taper model, timing on the STDS and MCT does not matter (e.g., Robinson et al., 2006). In contrast, both channel flow and wedge insertion models predict contemporaneous motion on the MCT and STDS, both in the hinterland and the klippen (Godin et al., 2006; Webb et al., 2011).

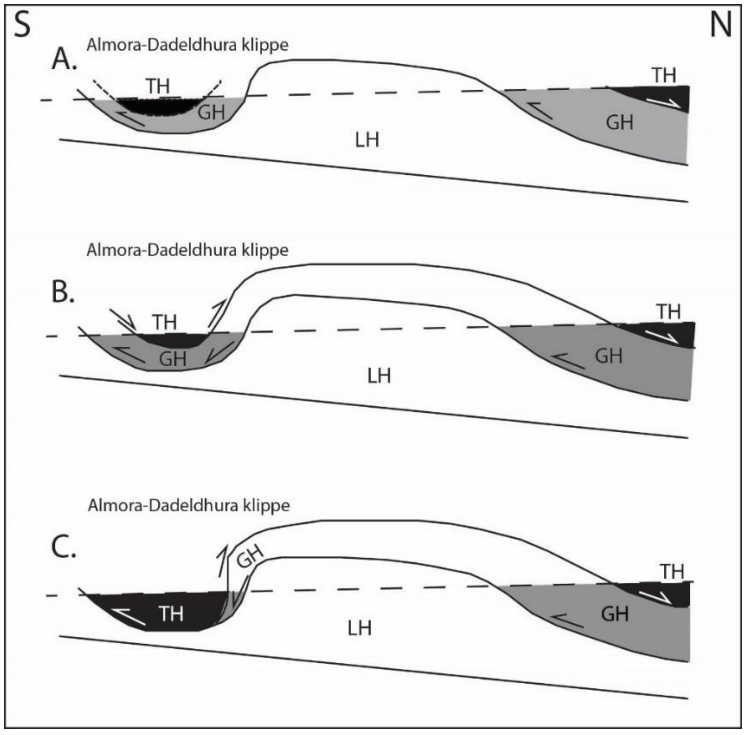

Figure 3. Contrasting tectonic models developed from the Almora-Dadeldhura klippe by recent studies. A. Critical taper (Gehrels et al., 2006) - klippe is composed entirely of Greater Himalayan rocks, with the Tethyan Himalayan rocks overlying Greater Himalayan rocks across an unconformity. The STDS is not present in the klippe; B. Channel flow (Antolín et al., 2013) - STDS is parallel to MCT and in the klippe. The klippe has Tethyan Himalayan rocks in the STDS hanging wall and Greater Himalayan rocks in the STDS footwall/MCT hanging wall; C. Wedge extrusion (He et al., 2016) - MCT and STDS merges under the klippe. The klippe is composed almost entirely of Tethyan Himalayan rocks, with a strip of Greater Himalayan rock between MCT and STDS, in the northern portion of the klippe.

Deviations from an idealized model are expected. For example, researchers report both pure shear and simple shear in Greater Himalayan rocks (e.g., Grujic et al., 1996; Long et al.,

2016). The absence of the STDS in the klippe does not necessarily disprove channel flow or wedge insertion models because the fault may have been eroded. Younger cooling ages to the north can be explained by out-of-sequence thrusting, or presence of a thrust ramp, which can cause late exhumation, or late phase structural deformation in response to further shortening towards the foreland.

4. GEOLOGY OF THE ALMORA-DADEKDHURA KLIPPE

The Almora-Dadeldhura klippe is composed of metamorphosed rocks with a generally right way up metamorphic grade and a shear zone surrounding the klippe (Valdiya, 1980). Underneath the klippe, the Ramgarh-Munsiari thrust carries Paleoproterozoic Lesser Himalayan rock, and is folded into a syncline with the overlying Greater Himalayan rock (Robinson et al., 2006; Mandal et al., 2014). Tethyan Himalayan rocks are present in the core of the syncline in Nepal. Presently, the klippe is an eroded syncline, with the axis trending WNW-ESE (Figure 4). In India, the klippe shows repetition of lithologies on both limbs of the fold (Valdiya and Kotlia, 2001).

In Nepal, the klippe rocks are divided into two stratigraphic units based on their metamorphic grades, the Bhimphedi Group and Damgad Formation, (Kaphle, 1992). The Bhimphedi Group is composed of medium to high grade metasedimentary rocks with Neoproterozoic protoliths intruded by Cambrian-Ordovician granite (DeCelles et al., 1998; Johnson et al., 2001). The Damgad Formation is composed of low-grade to unmetamorphosed sedimentary rocks of Ordovician-Devonian age (Stöcklin, 1980; Upreti, 1999). The Damgad Formation is correlated with the Phulchauki Group in central Nepal, which is correlated with the lower Paleozoic Tethyan Himalayan rocks (Stöcklin, 1980). The Bhimphedi Group have a Greater Himalayan affinity (Robinson et al., 2006; Mandal et al., 2014). In the Almora klippe,

the estimated metamorphic temperatures range from 300-709 ºC, pressures are 6-8 kbar and show a decreasing up-section metamorphic grade (Figure 5; Srivastava and Mitra, 1994; Joshi and Tiwari, 2009). In India, klippe rocks are metamorphosed to amphibolite facies with garnet-mica schist, schist, quartzite and augen gneiss (Valdiya, 1980; Mandal et al., 2014). In Nepal, temperatures decrease from 500-650 ºC to 300-400 ºC towards the center of the klippe, as estimated from quartz recrystallization textures (Figure 5; Antolín et al., 2013). In India and Nepal, the klippe has Cambrian-Ordovician intrusive granites; however, these granites are not present in the Damgad Formation (Trivedi et al., 1984; Kaphle, 1992; Gehrels et al., 2006).

5. PUBLISHED STUDIES

All recent studies from the Almora-Dadeldhura klippe agree that the Almora-Dadeldhura shear zone is the southern extension of MCT or some Greater Himalayan fault (e.g., Robinson et al., 2006; Antolín et al., 2013; Carosi et al., 2013; Montomoli et al., 2013; Mandal et al., 2014; La Roche et al., 2016). Detrital zircon age populations and εNd values of the klippe rocks (Bhimpedi Group) establish them as Greater Himalayan rocks (DeCelles et al., 2000; Robinson et al., 2001; Gehrels et al., 2006; Mandal et al., 2014) and top-to-the-south shear sense of the Almora-Dadeldhura shear zone (Srivastava and Mitra, 1994; He et al., 2016) conforms with this inference.

5.1 West Almora-Dadeldhura klippe, Bageshwar, Chaukhutia and Someshwar road transects, India

Metamorphic grades in the Almora-Dadeldhura klippe along the Kausani and Bageshwar transect (Transect A in Figure 4) generally decrease up stratigraphic section from the base of the klippe (Joshi and Tiwari, 2009). However, the change in metamorphic grade is limited (600-450 ºC), which can be attributed to the similar bulk rock compositions of the protoliths (Joshi and

Tiwari, 2009). Rocks near the center part of the klippe, were not influenced by shearing on the basal shear zone and have temperatures of 500-709 ºC (Joshi and Tiwari, 2009). The rock units near the basal shear zone (equivalent to Bhimpedi Group in western Nepal) show evidence of over-printed metamorphism during shearing as the klippe was emplaced with temperatures of ~450 ºC (Joshi and Tiwari, 2009). After emplacement of the Greater Himalayan rocks, the metamorphic isograds were folded as the klippe was folded (Joshi and Tiwari, 2009). The shear zone bounding the klippe is a mylonitized granitic augen gneiss in the central portion of the klippe, which shows an inverted metamorphic temperature gradient within the shear zone. Metamorphic temperature in the Almora-Dadeldhura shear zone varies between 400 ºC at base to 500-600 ºC at top of the shear zone (Srivastava and Mitra, 1996).

The Almora-Dadeldhura shear zone has deformation temperatures of 400-600 ºC (Srivastava and Mitra, 1996). Feldspar in the mylonite were rigidly rotated during top-south shearing, and quartz grains were recrystallized, indicating shearing in the brittle regime (Srivastava and Mitra, 1996). Recent detrital zircon ages show a maximum depositional age of 580 Ma from rocks at the center of the klippe and 810 Ma from the rocks close to the Almora-Dadeldhura shear zone (Mandal et al., 2014).

5.2 Central Almora-Dadeldhura klippe, Dadeldhura road transect, far-western Nepal

In Nepal, the maximum depositional age of the Bhimpedi Group is 960 Ma, and the overlying Damgad Formation is 520-480 Ma (Gehrels et al., 2006). Based on U-Pb ages of cross-cutting, foliated granite (474±10 Ma and 512±11 Ma), a Cambrian-Early Ordovician tectonic event is identified in the Bhimpedi Group due to accretion along the northern margin of the Indian plate in Paleozoic time (Gehrels et al., 2006).

The contact between the Bhimpedi Group and Damgad Formation shows that foliations in the Bhimpedi Group have a cross-cutting relationship with the overlying, lower conglomerate unit of the Damgad Formation (Gehrels et al., 2006). From the cross-cutting relationship, age difference and metamorphic history, Gehrels et al. (2006) interpret the contact as originally an angular unconformity, which was sheared during Tertiary deformation. The bedding planes of the underlying phyllite and quartzite of Bhimpedi Group trace into the overlying conglomerate of Damgad Formation at a high angle. The Bhimpedi Group was interpreted to have the maximum depositional age of 960 Ma and the Damgad Formation was interpreted to be deposited between 520-480 Ma (Gehrels et al., 2006). In the contact between the Bhimpedi Group and Damgad Formation, the early prograde metamorphism has relict kyanite grains, while a retrograde, chlorite-grade metamorphism documents the Tertiary deformation (Næraa et al., 2007). Chlorite grains in the contact define a top-north S-C fabric, formed during the Tertiary deformation (Næraa et al., 2007).

Antolín et al. (2013) use quartz recrystallization textures to estimate metamorphic temperatures across the klippe and compiled available temperature data from Naeraa et al. (2007, Gt-Bt thermometry) and Beyssac et al. (2004, Raman Spectroscopy). Their estimates show 400-650ºC metamorphic temperatures in the Bhimpedi Group and 300-500ºC temperatures in the overlying Damgad Formation (Figure 5). A muscovite cooling age near the Almora-Daddeldhura thrust is 22.7±0.7 Ma (425 ºC closing temperature, Antolín et al., 2013). The sheared contact between the Bhimpedi Group and Damgad Formation has younger muscovite cooling ages between 16-18 Ma (275-425 ºC closing temperature, Antolín et al., 2013). Antolín et al. (2013) correlate these ages with motion on the STDS. However, the muscovite cooling ages could record the time when the klippe rocks were moved along the MCT, or another intra-Greater

Himalayan thrust, toward the surface of the Earth. The slightly younger ages of the sample from the contact of Bhimpedi Group and Damgad Formation may be due to the lower closing temperature of the muscovite samples collected from this location because the size of the grains are smaller (<2 µm, 275-425 ºC, Wemmer and Ahrendt, 1997) compared to those collected from the basal shear zone (500 µm, 425 ºC, Harrison et al., 2009).

The estimated metamorphic temperatures of the Bhimpedi Group and the Damgad Formation does not have a conspicuous contrast across the contact between the two units. Although the temperatures range between 300-650 ºC, rocks on either side of the contact have metamorphic temperatures overlapping between ~350-500 ºC (Figure 4 in Antolín et al., 2013). A generally decreasing up-section, from north-south, trend of metamorphic grade from garnet-mica schist to grey phyllite exists (Upreti and LeFort, 1999). The difference in the metamorphic history of the Bhimpedi Group and Damgad Formation, and overprinted microstructures, defined by chlorite grains in the contact, suggest that this contact was initially an unconformity, which was sheared in a late top-north deformation event. Antolín et al. (2013) suggest that the sheared contact between the Bhimpedi Group and Damgad Formation is the STDS, which ceased movement at 17 Ma. However, this age is not coeval with hinterland STDS ages. Cross-cutting granite ages north of the Almora-Dadeldhura klippe shows that deformation along the STDS ceased by 25-23 Ma (Bura-Buri, western Nepal, Carosi et al., 2013). Because, no temperature jump exists, a mismatch in timing exists and the shear zone could have formed when the Almora-Dadeldhura syncline formed after the emplacement of the MCT sheet, I suggest that the Bhimpedi/Damgad contact is not the STDS. The contact can be interpreted as an unconformity between the Greater Himalayan rocks and Lesser Himalayan rocks and was sheared during the Tertiary orogeny.

5.3 Eastern Almora-Dadeldhura klippe, Karnali and Tila River section, western Nepal

The Bhimpedi Group has an increasing up-section metamorphic grade, ranging from biotite to kyanite grade (Upreti and Le Fort, 1999). In contrast, the Damgad Formation is composed of calcareous metasedimentary rocks to limestone that are metamorphosed to greenschist facies, and has decreasing up-section metamorphic grade (Upreti and Le Fort, 1999). In this region, the Karnali shear zone is the contact between the Bhimpedi Group and Damgad Formation. An in-situ monazite sample from the Karnali shear zone shows a prograde metamorphic history with garnet growth from 36-30 Ma (LaRoche at al., 2016). At 30 Ma, prograde metamorphism ceased after attaining 600ºC and was followed by a retrograde phase from 30-24 Ma (LaRoche at al., 2016). Muscovite grains are 350 μm with a 450–480 °C closing temperature and yield an age of 19 Ma from the Karnali shear zone (LaRoche et al., 2016).

16 Apatite Fission Track (AFT) ages are available from the Indian portion of the Almora-Dadeldhura klippe, which range between 3.7±0.8 to 13.1±0.6 Ma (Patel et al., 2015). These AFT ages show a pattern which can be correlated with the structures in the klippe (see discussion in chapter 7.3). AFT ages from the Karnali River have cooling ages of 10-4 Ma (van der Beek et al., 2016), do not have a pattern, and are slightly younger than the AFT ages in India (~13-4 Ma, Patel et al., 2015). These data do not show any linear correlation with elevation, which indicates that the AFT ages are unlikely to be influenced by erosion.

The 36-30 Ma ages of prograde metamorphism in the Karnali shear zone record burial of the Bhimpedi Group (Greater Himalayan rocks) by the Tethyan thrust belt as it propagated southward. The retrograde 30-24 Ma metamorphic ages represent the onset of thrusting along the Almora-Dadeldhura shear zone (LaRoche et al., 2016), which was the first movement recorded

in the basal shear zone of the Almora-Dadeldhura klippe. The 19 Ma muscovite cooling ages from the same horizon indicate the last phase of exhumation related cooling through ~450ºC.

The Almora-Dadeldhura shear zone is 1200 m thick with the Tila shear zone to the south (Figure 2; He et al., 2016). The metamorphic rocks between the Almora-Dadeldhura and Tila shear zones are kyanite-bearing paragneiss and calc-silicate with orthogneiss interlayers, which He et al. (2016) identify as Greater Himalayan rocks. He et al. (2016) state that the rocks south of the Tila shear zone are comparatively less metamorphosed with the metamorphic grade decreasing up section, are intruded by Cambrian-Ordovician granites, and designate them as Tethyan Himalayan rocks. This is a different interpretation as most other workers identify these rocks as Greater Himalayan (e.g., LaRoche et al., 2016).

Cross-cutting leucogranite ages of the Tila shear zone indicate motion ceased by 17-14 Ma (He et al., 2016), which is interpreted as the STDS. If this fault was the STDS, its age is much different than the age of movement on the STDS, north of the Almora-Dadeldhura klippe at 25-23 Ma, based on the emplacement of leucogranite, that cross-cuts the STDS (Carosi et al., 2013). The Tila shear zone is 6-11 million years younger than the nearby STDS ages; thus, the Tila shear zone is likely not the STDS. If the rocks are Greater Himalayan, the Tila shear zone is an intra-Greater Himalayan shear zone.

In the same transect, different data results in completely different interpretations. In the Tila River section, He et al. (2016) correlate the Tila shear zone with the STDS because top-north with a few top-south shear sense indicators are present and it separates an inverted metamorphic gradient in footwall, from a right way up metamorphic gradient in the hanging wall. He et al. (2016) report the Karnali shear zone as a local sheared contact, citing the change in rock type across the Karnali shear zone as unimportant. In contrast, LaRoche et al. (2016)

report only top-south shear sense indicators in the Tila shear zone, no top-north, designating it as a local shear zone, because of the similarity in metamorphic grade on either side of the shear zone. LaRoche et al. (2016) correlate the Karnali shear zone with the STDS, because of the conspicuous change in rock type across the shear zone from greenschist to amphibolite facies metamorphic rocks, to overlying weakly to non-metamorphosed calcareous sedimentary rocks.

Two different studies result in two different interpretations for the same rocks, in which the two resulting papers advocate for two different models. LaRoche et al. (2016) advocate the channel flow model while He et al. (2016) advocate the wedge insertion model. I can take the same data from the Karnali and Tila shear zones and advocate for the critical taper model. In the context of the critical taper model, the Tila shear zone could be either the Almora-Dadeldhura thrust or an intra-Greater Himalayan thrust as LaRoche et al. (2016) report dominantly top-south shear sense indicators. The Karnali shear zone is the Bhimphedi/Damgad contact and could be a localized fault from folding or emplacement of the klippe.

6. METHODS

Field work was done on foot and by car, in and around the Almora-Dadedldhura klippe along 3 transects in India and 1 transect in far western Nepal (Figure 4). The basal shear zone of the Almora-Dadeldhura klippe was examined at multiple locations wherever accessible. Most of the exposures examined were present along road cuts, with a few exceptions of river sections. Exposures were not continuous, and often not workable due to extensive weathering in this humid and highly vegetated region of the Himalayas, making it difficult to trace shear zones and contacts across the thrust belt. Dip and strike measurements were taken at all exposures where an identifiable foliation was present. Shear sense indicators were studied from sections trending perpendicular or within 20º of the perpendicular to the strike direction. Shear sense indicators

were identified and noted along with the section orientation and a GPS waypoint (Figures 5 and 6).

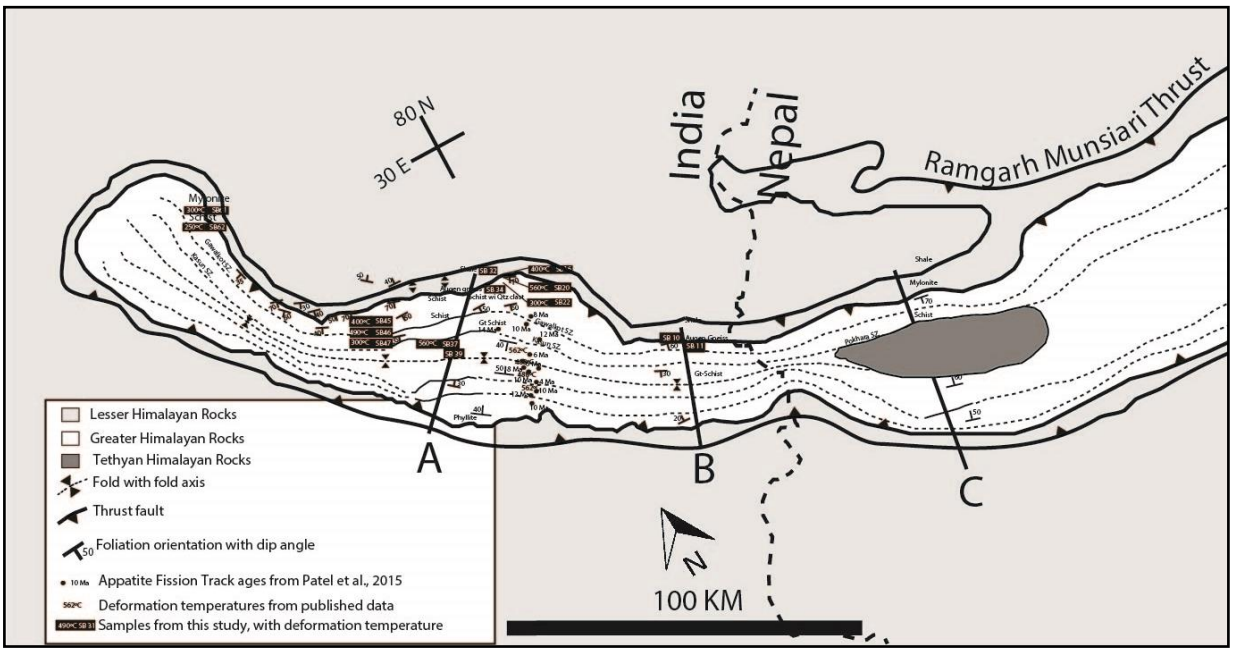

Figure 4. Geological map of the Almora-Dadeldhura klippe with data points and sample locations.

Figure 5. Field photograph of outcrops. Left photo (SB 32, 29.7774º N, 79.6076º E) of red shale in the Lesser Himalayan sequence underlying the Almora-Dadeldhura klippe. Right photo (SB 20, 29.7410º N, 79.7169º E) is a feldspar clast in the augen gneiss of the Almora-Dadeldhura Shear zone showing a tail formed due to a top south shearing. Section is oriented 200º-20º.

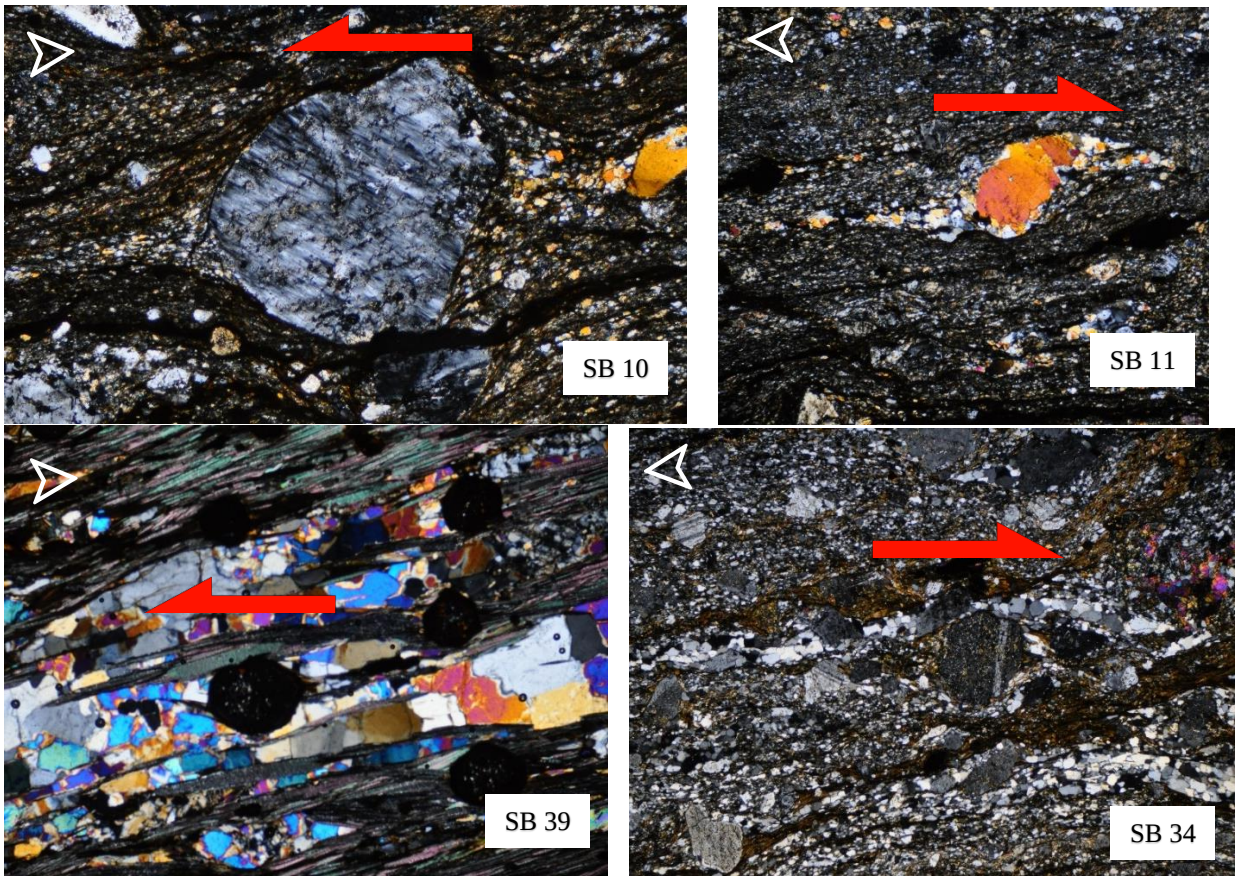

Figure 6. Representative microscopic shear sense indicators. Location of samples in Figure 16. SB 10 shows rigid rotation of feldspar clast. SB 11 is a sigma type shear sense indicator. SB 39 is a delta type shear sense indicator. SB 34 is a poorly formed sigma type shear sense indicator. White arrowheads point indicated north.

Oriented samples were collected from rock units with foliation. Orientation of the major foliation plane was marked on the exposed foliation surface (Figure 7) before breaking the sample out from the main outcrop. XZ oriented thin sections were prepared at the facility at Presidency University, Kolkata India. X, or the direction of stretching was assumed parallel to the dip direction of the foliation based on Anisotropic Magnetic Susceptibility (AMS) of one representative sample (see discussion below). This assumption matches with the assumption made by Srivastava and Mitra (1996) who worked in the same area. Arrows pointing along the dip direction of the foliation was transferred onto the thin section glass, after cutting the sample, and then was polished (Figure 8). Some of the thin sections were scanned and stitched into a

high-resolution mosaic using the Carl Zeiss automated microscope facility at the Fabric Analysis Laboratory at the Indian Institute of Technology (example Figure 9).

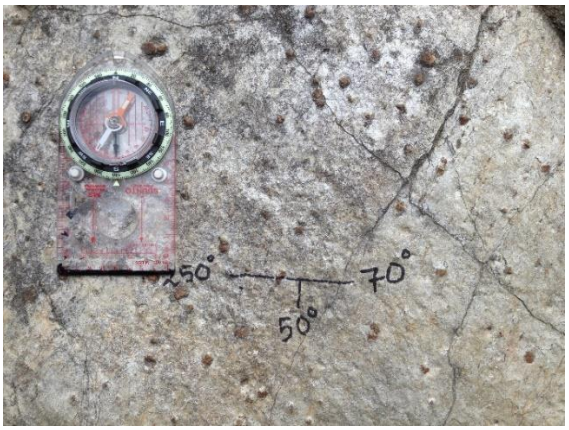

Figure 7. Foliation orientation marked on the outcrop before breaking up the sample.

Figure 8. Method of transferring dip direction of foliation on thin section before polishing. Arrowhead towards top of the sample.

An oriented augen gneiss sample (SB 139) was picked from the Almora-Dadeldhura shear zone, which had the maximum abundance of quartz amongst the collected oriented samples, for EBSD analysis. EBSD analysis of the quartz grains was done at the EBSD facility of the Indian Institute of Technology, to estimate a- and c- axes orientation of quartz grains for strain analyses of the sample. Due to the absence of any identifiable stretching lineation in the thin section, a core was extracted from this sample (Figure 10) for Anisotropic Magnetic Susceptibility (AMS) analysis, from which the elongation direction of the microfabric was estimated. The elongation direction was estimated to be 42º→150º, which is parallel to the dip direction of the foliation in the sample (46º→150º).

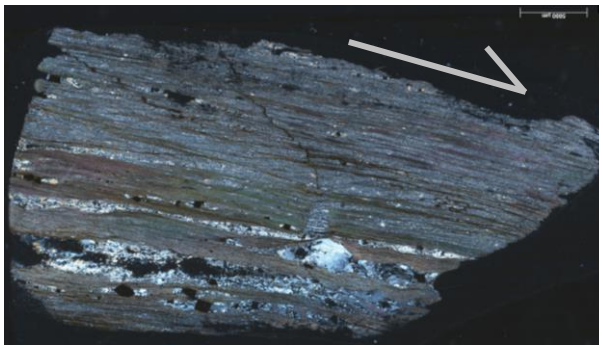

Figure 9. High resolution mosaic scan of entire thin section under cross-polar. Arrow represent dip direction of the sample 40º→210º. Arrow head towards the top of the sample.

Figure 10. Core extraction from oriented sample for AMS analysis. Blue arrowhead showing dip direction in sample.

A thin section was prepared along the XZ plane, containing the elongation direction, for EBSD analysis. EBSD analysis yielded weak asymmetry of the a-axes and weak Crystal Preferred Orientation (CPO) of the c-axes (Figure 11). CPO map of the quartz grains in the thin section also did not yield an identifiable color-coding pattern (Figure 12). This can be due to the recrystallisation of the quartz grains after the shearing in the Almora-Dadeldhura shear zone.

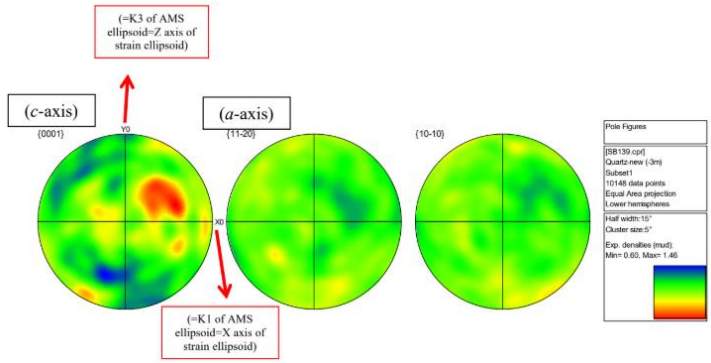

Figure 11. Equal area lower hemisphere projection of quartz c- and a-axes from sample SB 139. K3 and K1 is the X and Z axis respectively, determined from the AMS data of a core from the same sample.

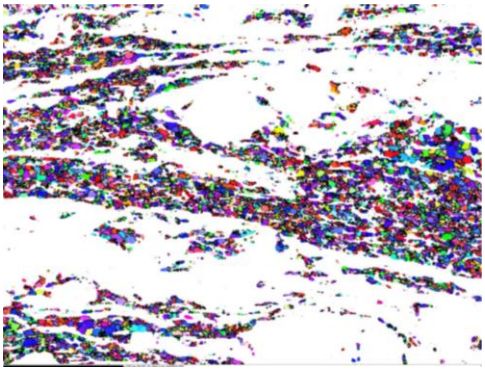

Figure 12. Inverse Pole Figure (IPF) coloring map of quartz grains from sample SB 139.

Semi-quantitative thermometry from dynamically recrystallized quartz was done from 9 samples. Following the method described by Stipp et al. (2002), the dominant recrystallization

mechanisms in each of the thin sections were interpreted from quartz microstructures and was used to estimate semi-quantitative deformation temperature (Table 2., Figure 14 and 15). Law (2014) calibrated the temperature estimations by Stipp et al. (2002) for bulging, subgrain rotation, and grain boundary migration recrystallization for Himalayan rocks. Strain rate in the analyzed samples are assumed to be in the same range as described by Stipp et al. (2002) and Law (2014, 10^{-12}-10^{-14} sec-1). The samples were collected from 3 different transects, and one from the center of the Almora-Dadeldhura klippe (Figure 4).

7. DATA AND INTERPRETATION

7.1 Correlating shear zones from different transects

The shear zone bounding the klippe in the north is 2200 m wide in India (Srivastava and Mitra, 1996, this study), and is a sheared garnet mica schist, while ~3000 m wide at the eastern end of the klippe in Nepal where the base of the shear zone is garnet mica schist and the top of the shear zone is a paragneiss with mylonitic calc-silicate (He et al., 2016). From the Indian portion of the Almora-Dadeldhura klippe, the northern parts of the shear zones are interpreted to be top-north, while southern parts of the same shear zones are reported to be top-south (Transects A and B in Figure 12; Joshi and Tiwari, 2009; Patel et al., 2015). In Nepal, both the northern and southern parts of the shear zones are interpreted as top-south (e.g., Robinson et al., 2006). Inside the klippe in Nepal, the sheared contact between the Bhimpedi Group and Damgad Formation in the west and the Karnali shear zone in the east is the contact between Greater Himalayan and Tethyan Himalayan rocks. These two shear zones are interpreted as top-north in both southern and northern flanks of the klippe (Transect B, Figure 13; Antolín et al., 2013; LaRoche et al., 2016). In the Tila shear zone to the NE of the Almora-Dadeldhura klippe (Transect C, Figure

13), He et al. (2016) interpret the contact as top-north, with a few top-south shear indicators, while LaRoche et al. (2016) interpret exclusively top-south shear sense indicators.

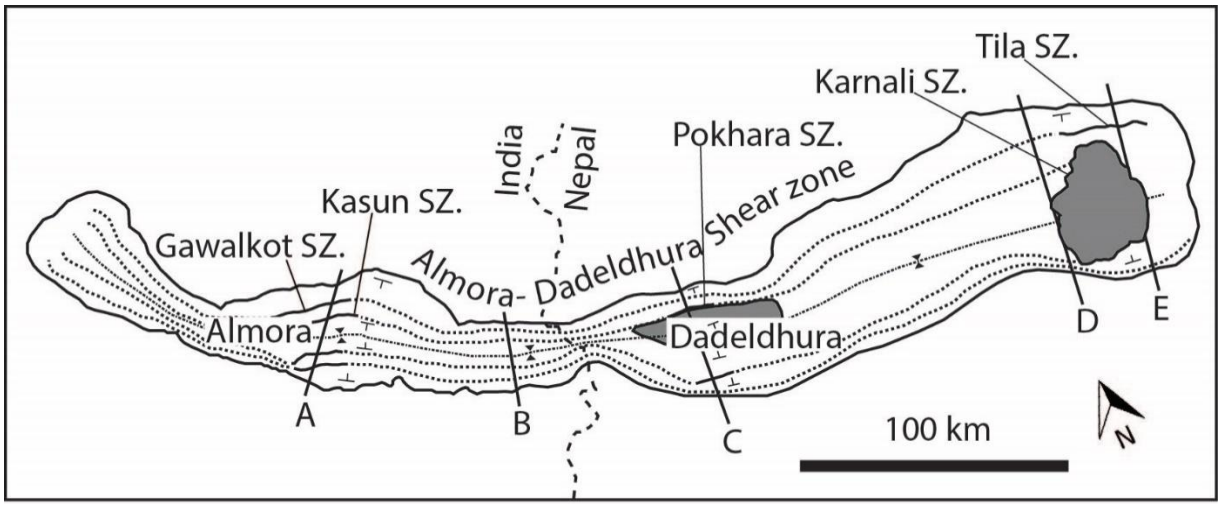

Figure 13. Map of the shear zones in the Almora-Dadeldhura klippe. The map shows the major shear zones in the klippe as reported by different studies (solid line),and correlated across the klippe (dotted lines) by this study. A. Srivastava and Mitra (1996), Valdiya and Kotlia (2001), Joshi and Tiwari (2009), Patel et al. (2015), Mandal et al. (2016); B. Næraa et al. (2007), Antolín et al. (2013); LaRoche et al. (2016); Upreti and LeFort, 1999; C. He et al. (2016). Box with black outline shows location of Figure 15.

The angular unconformity between the Damgad Formation and the Bhimpedi Group in transect B was overprinted during Tertiary deformation (Gehrels et al., 2006) and is now a sheared unconformity, 6000 m vertically above the Almora-Dadeldhura shear zone (Gehrels et al., 2006). Antolín et al. (2013) interprets the same contact as the STDS with top-north shear with a vertical separation of 6600 m from the Almora-Dadeldhura shear zone. The 600 m mismatch in the vertical separation is possibly due to errors in measurement of the vertical distances from published low resolution cross-sections.

Use of different nomenclature and criteria to define these shear zones complicates their correlation across the klippe. Because the klippe structure is consistent along strike, stratigraphic separation can help to correlate shear zones from different transects. Table 1 shows the correlation of different shear zones based on their vertical separation from the Almora-

Dadeldhura shear zone. These shear zones crop out on both limbs of the Almora-Dadeldhura synform. Only the shear zone names from the northern flank of the klippe are used for simplicity.

Table 1. Comparison of Vertical Separations of shear zones from different transects

Kausani transect (A)		Dadeldhura transect (B)		Karnali transect (C)	
Shear zone	Separation	Shear zone	Separation	Shear zone	Separation
Kasun	[1]6 km	Pokhara	[2]6.6 km	Karnali	[3]6.2 km
Gwalakot	[1]2.5 km	-	-	Tila	[4]1 km (Variable)

[1] Valdiya and Kotlia (2001, Figure 2); [2] Antolín et al. (2013, Figure 8d); [3] LaRoche et al. (2016, Figure 1b); [4] He et al. (2016, Figure 6b).

From quartz c-axes, Joshi and Tiwari (2009) interpret that the Almora-Dadeldhura shear zone had late phase top-north shear in the northern limb, and top-south shear in the southern limb. The top-north shear shows plain strain to flattening strain conditions. Similar quartz c-axes patterns indicating pure shear existed in far western Nepal (Antolín et al., 2013; He et al, 2016; LaRoche et al., 2016).

7.2 Quartz recrystallization thermometry

Augen gneiss samples SB 16, SB 20 and schistose sample SB 22 were collected from the Almora-Bageshwar road transect near Takula village (Figure 4). Figure 14 shows a microscopic picture from each sample. SB 16 has sutured grain boundaries and sparse bulges along the grain boundaries, indicating a maximum deformation temperature of 400 ºC. The quartz grains were fractured, and the larger grains showed undulose extinction. SB 20 has grain boundary migration, with biotite grains cutting into the quartz grain boundary in several grains, indicating maximum deformation temperature of 560 ºC. Undulose extinction and grain boundary migrations are also present. SB 22 shows undulose extinction in the quartz grains, indicating maximum deformation temperature of 300 ºC. SB 37 was a standalone phyllite sample from the center of the klippe, and

showed irregular grain shapes with signs of grain boundary migration, indicating a maximum deformation temperature of 560 ºC.

Augen gneiss samples SB 45, SB 46 and SB 47 were collected from the Someshwar road transect (Figure 4). SB 45 shows weak foliation formed by quartz grains in the groundmass, indicating maximum deformation temperature of 400 ºC. SB 46 shows undulose extinction in quartz grains with sutured grain boundaries, indicating maximum deformation temperature of 490 ºC. The larger quartz grains are fractured and shows undulose extinction. SB 47 was furthest from the Almora-Dadeldhura shear zone and shows undulose extinction in fractured quartz grains, indicating a maximum deformation temperature of 300 ºC.

Phyllitic schist samples SB 61 and SB 62 are collected near the western end of the Almora-Dadeldhura klippe (Figure 4). SB 61 shows undulose extinction in fractured quartz grains, indicating a maximum deformation temperature of 300 ºC. SB 62 shows fractured quartz grains with bulges along the grain boundaries, indicating a maximum deformation temperature of 250 ºC.

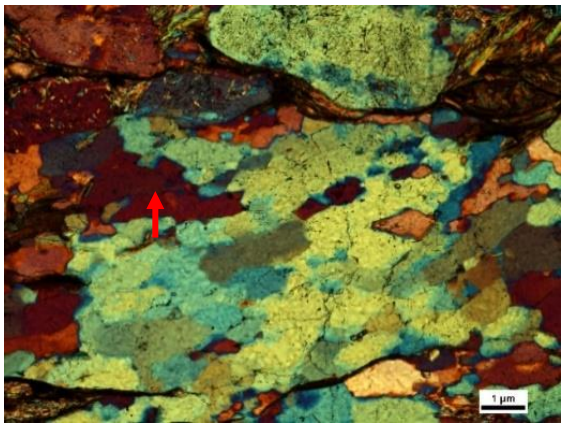

SB 16. Sutured grain boundaries and bulges (arrow). Maximum deformation temperature of 400 ºC.

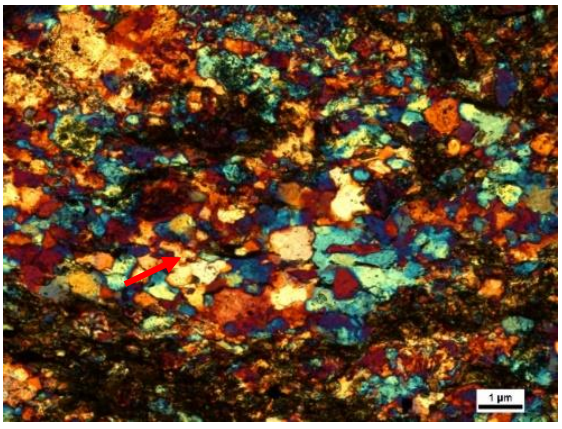

SB 20. Grain boundary migration, Irregular grain shape, biotite intrusion in quartz grain (arrow). Maximum deformation temperature of 560 ºC.

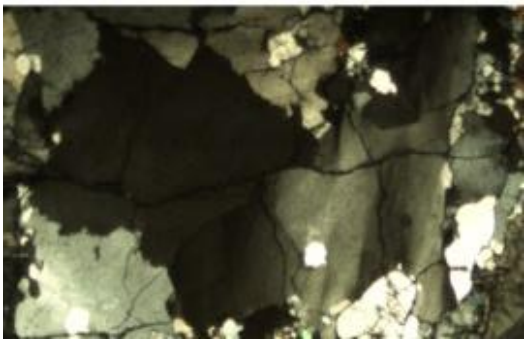

SB 22. Undulose extinction in quartz grains. Maximum deformation temperature of 300 ºC.

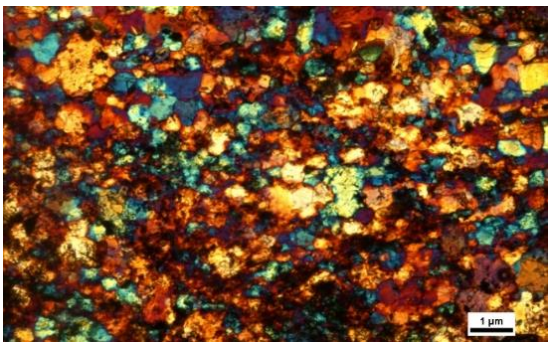

SB 37. Irregular grain shape due to grain boundary migration. 560 ºC.

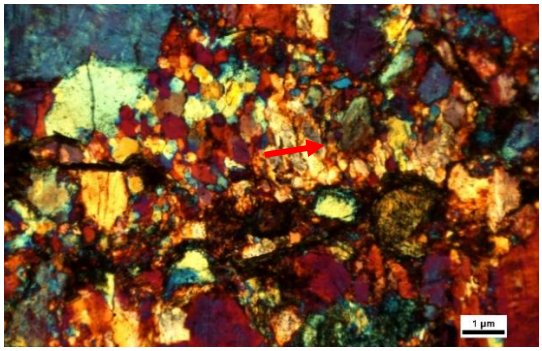

SB 45. Recrystallized grains with sutured grain boundaries (arrow). Maximum deformation temperature of 400 ºC.

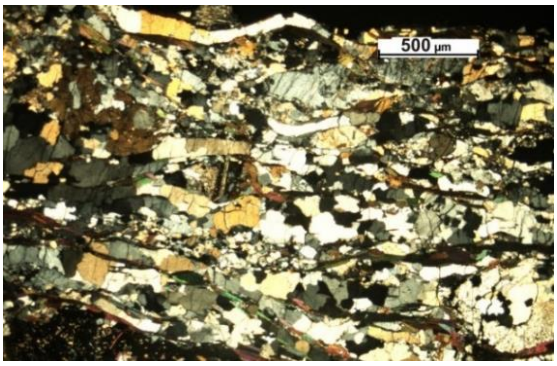

SB 46. Elongated quartz grains forming weak foliation. Maximum deformation temperature of 490 ºC.

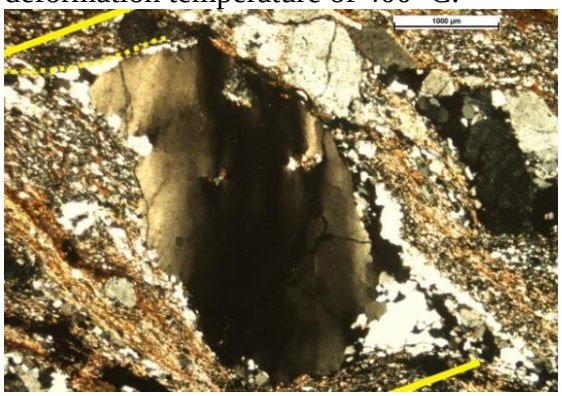

SB 47. Undulose extinction in quartz grain. Maximum deformation temperature of 300 ºC.

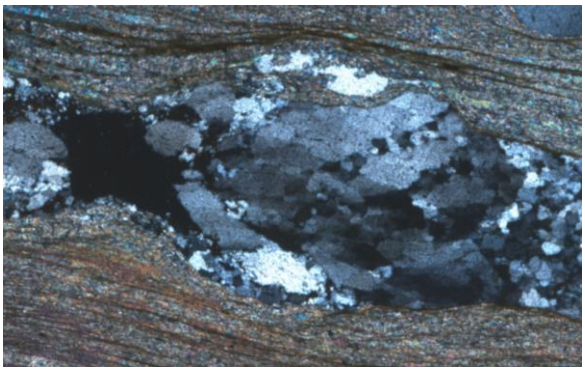

SB 61. Undulose and patchy extinction in quartz grain. Maximum deformation temperature of 300 ºC.

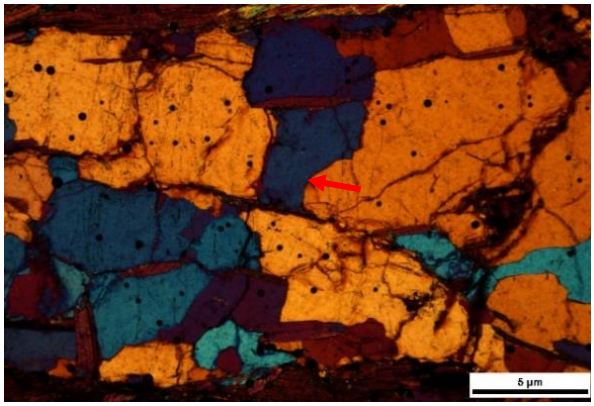

SB 62. Fractured grains, bulges (arrow) along grain boundary. Maximum deformation temperature of 250 ºC.

Figure 14. Quartz recrystallization microstructures in samples from the Almora-Dadeldhura klippe. Sample number, index microstructures and estimated deformation temperatures are described in individual figure captions.

Table 2. Deformation temperatures estimated from microtextures in samples collected from the Almora-Dadeldhura klippe (Figure 14). See Figure 15 for sample locations.

Sample	Micro-texture defining deformation temperature	Temp.	Lat	Long
SB 16	Sutured grain boundaries and bulges.	400 ºC	29.7415º	79.7198º
SB 20	Grain boundary migration biotite intrusion in grain boundary.	560 ºC	29.741º	79.7169º
SB 22	Undulose extinction.	300 ºC	29.7378º	79.7141º
SB 37	Irregular grain shape, grain boundary migration.	560 ºC	29.7257º	79.6172º
SB 45	Recrystallization and sutured grain boundaries.	400 ºC	29.7746º	79.4621º
SB 46	Elongated grains forming weak foliation	490 ºC	29.7708º	79.4531º
SB 47	Undulose extinction	300 ºC	29.7739º	79.4480º
SB 61	Undulose extinction	300 ºC	30.0926º	79.2672º
SB 62	Fractured grains, bulges along grain boundary.	250 ºC	30.0973º	79.2588º

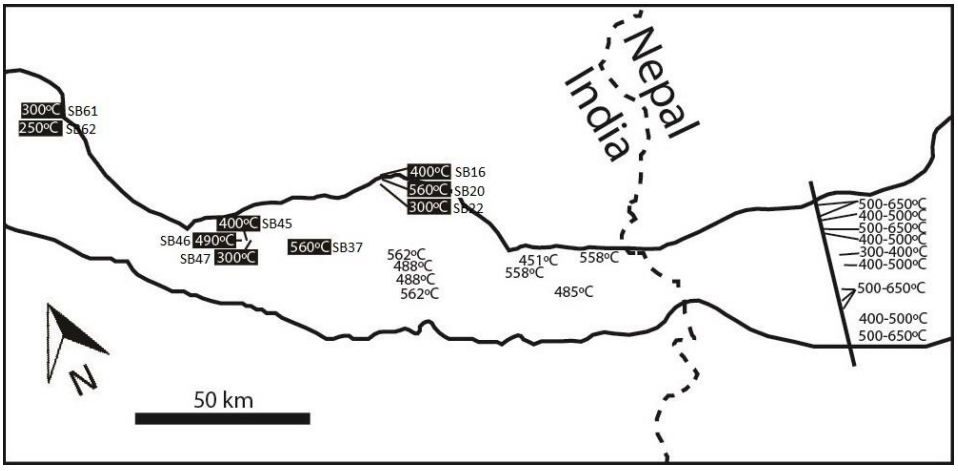

Figure 15. Metamorphic temperatures across the Almora-Dadeldhura klippe. Temperature estimations from Rawat and Sharma (2011, in India), Antolín et al. (2013, in Nepal), and this study (black box, in India).

7.3 Reinterpretation of published Apatite Fission Track (AFT) cooling ages

16 Apatite Fission Track (AFT) ages range between 3.7±0.8 to 13.1±0.6 Ma with the youngest ages are observed on the northern ends of the hanging walls of Kasun thrust (see Figure 13) and Almora-Dadeldhura shear zone (Patel et al., 2015). For example, at the northern outcrop of Kasun thrust, the hanging wall block has cooling ages of 3.9±0.5 Ma and 3.7±0.8 Ma, while the adjacent footwall block has cooling age of 12.2±0.6 Ma (Figure 13). Similarly, near the north Almora-Dadeldhura shear zone, cooling ages decrease towards the north on the hanging wall block (Figure 13). Although AFT ages usually record erosional exhumation along with tectonic uplift, these AFT ages do not show a linear correlation with elevation, indicating that these ages document cooling caused only by tectonic uplift (Patel et al., 2016).

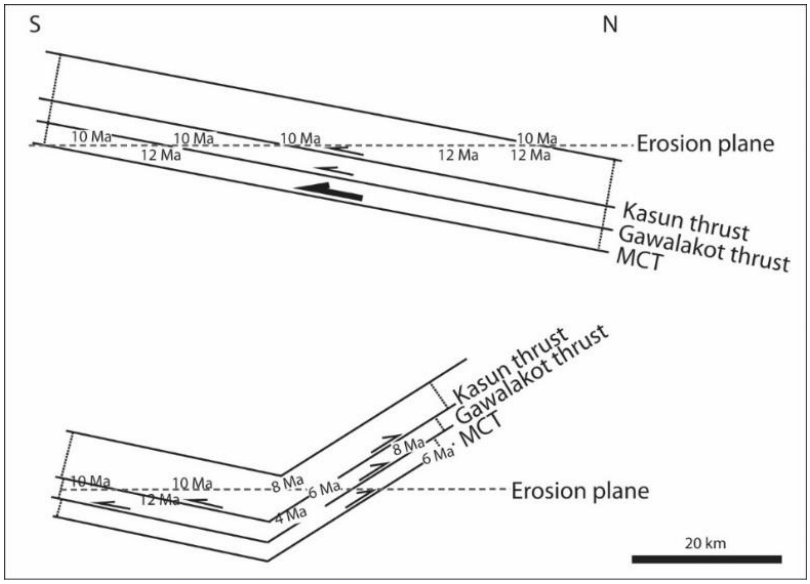

Figure 16. Reinterpretation of AFT cooling from Patel et al. (2016). Ages are presented after approximation to nearest even number for ease of visualization. 12-10 Ma ages are present across the klippe which represent the onset of exhumation when the klippe was emplaced along MCT. The younger cooling ages of 8-4 Ma are concentrated in the hanging walls of the flexural thrusts in the northern limb of the Almora-Dadeldhura syncline. These flexural thrusts were active when the syncline formed. The southern limb was not uplifted during the folding. Thus, the younger ages are found only in the northern limb.

Nine Zircon Fission Track (ZFT) ages range between 13.4 ± 0.6 and 21.4 ± 0.9 Ma (Singh and Patel, 2016). A pattern similar to the AFT ages is observed in the ZFT data. Younger ages are present on the northern limb, with a linear increase (R^2=0.6) in age towards south. The shear zones in the klippe did not affect the ZFT ages, because their activity happened after the klippe went through ZFT closure temperature.

The younger AFT ages in the northern limb of the Almora synform was likely caused when the klippe was folded by the emplacement of the younger Lesser Himalayan duplex, indicating an age of 4-8 Ma for folding (Figure 16). The southern limb retained the original ages from motion on the Almora-Dadeldhura thrust (Figure 16). During this folding, weak horizons in the klippe preferentially accommodated flexural slip, namely the contact between the Almora-Dadeldhura thrust and the klippe rock, Gwalkot thrust and Kasun thrust. These late, local shear zones remained active through Holocene time as documented by neotectonic geomorphic features (Valdiya and Kotlia, 2001). This late phase deformation took place in brittle regime, which is documented by the rigid rotations of the feldspar clasts in the top horizon of the Almora-Dadeldhura shear zone.

8. VALIDATING A TECTONIC MODEL

The channel flow model necessitates that the MCT and STDS be coeval. Antolín et al. (2013) and LaRoche et al. (2016) argue that within the Almora-Dadeldhura klippe the Damgad-Bhimpedi contact is the STDS and was active until 17 Ma. Antolín et al. (2013) cited hinterland-STDS ages from central Nepal as contemporaneous with this event, which is about 200 km east of the Almora-Dadeldhura klippe (Godin et al., 2006). Cross-cutting granite ages north of the Almora-Dadeldhura klippe shows that deformation along the STDS ceased by 25-23 Ma (Bura-Buri, western Nepal, Carosi et al., 2013). Even if the Damgad-Bhimpedi contact represents a

fault, this discordance in age does not allow this sheared contact to be correlated with STDS. Similar temperatures of 300-600 ºC on either side of the Pokhara shear zone and the peak deformation temperature of 400-500 ºC indicates that it is not a large scale regional shear zone (see section 5; Joshi and Tiwari, 2009; Gehrels et al., 2006).

The wedge insertion model requires the merging of the interpreted STDS with the MCT north of the klippe in the Tila shear zone (He et al., 2016). The interpreted STDS separates an inverted metamorphic sequence in the footwall from a lower metamorphic grade in the hanging wall, has cross-cutting granite intrusions, and top-north shear sense indicators (He et al., 2016). However, LaRoche et al. (2016) state that the Tila shear zone does not have any top-north shear indicators. The Tila shear zone and the Almora-Dadeldhura thrust can be interpreted as parallel from the structural data. The discordance of timing of between the shearing of the hinterland-STDS (25-23 Ma; Searle et al., 1999; Carosi et al., 2013) and interpreted-STDS (17 Ma, He et al., 2016) cannot be explained if the STDS is one continuous backthrust as implied by the wedge insertion model.

Data from the Almora-Dadeldhura klippe can be interpreted to support or refute each of the 3 models. Channel flow is not supported if the timing of the MCT and STDS are interpreted to be different. Wedge insertion is not supported if the STDS in the hinterland and klippe are the same fault but do not have motion at the same time. The critical taper model can accommodate the data from both of these studies. However, none of the faults in the klippe can be the STDS because the critical taper model views the STDS as a low angle fault that initiates in response to the high taper angle that results as the Himalayan thrust belt evolves (see Robinson and Pearson, 2013 for complete discussion). Thus, the STDS would not be a folded fault as the other models predict.

Table 3. Comprehensive review of available data for different tectonic models.

Data	Critical taper	Channel flow	Wedge insertion
Metamorphic temperatures decrease up-section in the klippe: 650-300ºC (Joshi and Tiwari, 2009; Antolin et al., 2013; Gehrels et al., 2006)	√	√	√
The bottom 3 km section has an inverted metamorphic gradient, which end at kyanite zone. This portion of the klippe has leucogranite intrusions (Upreti and LeFort, 1999; He et al., 2016).	√	√	√
Tila SZ ceased by 17-14 Ma, determined from cross cutting leucogranite (He et al., 2016).	√	X	√
In-situ monazite deformation temperature from Karnali SZ has 36-30 Ma pre-shear prograde metamorphism; 30-29 to <24 Ma syn-shear metamorphism. Muscovite cooling age, which show a time right after shearing ceased is, 19 Ma (LaRoche et al., 2016).	√	√	X
Pokhara SZ and Almora-Dadeldhura SZ have coeval muscovite cooling ages of 23-17 ma (Antolin et al., 2013). STDS ages from north of the klippe is 25-23 Ma (leucogranite, Carosi et al., 2013), which are not coeval with this age.	√	X	X
Quartz c-axes data from EBSD across the klippe. Shows top-south in the Almora shear zone. Plain strain to flattening strain regime deformation in the klippe. A late phase top-north shear interpreted from c-axes stereograms in northern flank of the klippe. (Joshi and Tiwari, 2009).	√	X	√
Microstructure shows rigid top-S rotation of feldspar porphyroclasts. EBSD data shows quartz crystals does not have CPO.	√	X	√
AFT ages from the klippe. range from 13-4 Ma. The younger ages are found only from the HW of the SZs, in the northern limb of the Almora synform (Patel et al., 2015).	√	√	√

9. KINEMATIC HISTORY OF THE KLIPPE: SUPPORT FOR THE CRITICAL TAPER MODEL

Greater Himalayan rocks were buried and experienced prograde metamorphism from 36-30 Ma (Figure 17. A, LaRoche et al., 2016) and experienced retrograde metamorphism between 30-24 Ma (Figure 17. B, LaRoche et al., 2016), which may be the result of intra-Greater Himalayan thrusts. Montomoli et al. (2013) documents motion on intra-Greater Himalayan thrusts at 28-18 Ma and motion on the MCT at 17-13 Ma north of the Tila and Karnali shear zones. An $^{40}Ar/^{39}Ar$

cooling age from further west in Greater Himalayan rocks is 25 Ma (Robinson et al., 2006); however, these ages could indicate Greater Himalayan rocks being brought to the surface on any of the Greater Himalayan thrusts including the MCT or recording cooling from another tectonic event. The MCT is emplaced with its Tethyan thrust belt overburden and moved southward over the underlying Lesser Himalayan rocks reached the present location of the Almora-Dadeldhura klippe between 22.9-19.6 Ma (Figure 17. C, Antolín et al., 2013). These klippe emplacement ages are from the Dadeldhura road transect. If these ages are translatable eastward along strike to the Karnali region, then the Almora-Dadeldhura shear zone may be from one of the intra-Greater Himalayan thrusts as these emplacement ages are more close to the 28-18 Ma ages from Montomoli et al. (2013). If these ages are not translatable along strike, it suggests that the MCT/Almora-Dadeldhura shear zone is diachronous along strike. Northeast of the Almora-Dadeldhura klippe, Montomoli et al. (2013) and Iaccarino et al. (2016) state an age of 17-13 Ma on the MCT. Between 22.9-19.6 Ma, the klippe was emplaced over the MCT, which exhumed and cooled the klippe rocks below muscovite closing temperature. The oldest AFT ages in India in the klippe are ~16 Ma (Patel et al., 2015), which probably reflect Greater Himalayan rocks cooling through the 100 ºC isotherm from emplacement along the MCT or another intra-Greater Himalayan thrust. The Ramgarh-Munsiari thrust sheet cooled through ~425 ºC isotherm between 17-7 Ma (Robinson et al., 2006), the cooling age spectra from this sample is disturbed. In Nepal, if the youngest age of the MCT is 13 Ma (Montomoli et al., 2013; Iaccarino et al., 2016), then the youngest age for motion on the Ramgarh-Munsiari thrust is 13 Ma. We know that in the Siwalik Group, the first appearance of detritus from Paleoproterozoic rocks carried by the Ramgarh-Munsiari thrust is about 11-10 Ma (Robinson et al., 2001). Faulting propogated southward through Lesser Himalayan rocks to build the Lesser Himalayan duplex (Figure 17. D).

In western Nepal, kinematic modeling shows that an age of 15 Ma for motion in the duplex was possible (Robinson and McQuarrie, 2012 and references therein). However, the 13 Ma age of motion on the Ramgarh-Munsiari thrust negate this age, unless the faults are diachronous along strike. The Main Boundary thrust south of the Almora-Dadeldhura thrust can be viewed as the last thrust in the duplex and has an age of first motion at ~4 Ma in central Nepal (Rösler et al., 1997; Ojha et al., 2009). If this age is translateable along strike, this yields motion on the Lesser Himalayan duplex from ~10-4 Ma. Thrust sheets within the Subhimalayan thrust system were emplaced after 4 Ma.

As the Lesser Himalayan duplex grew, the MCT was tilted to dip toward the north (Robinson et al., 2003) and the northern limb of the Almora-Dadeldhura klippe was tilted to dip toward the south (Figure 17. E). If the duplex grew from 14-5 Ma in Kumaon, this may have produced some of the young AFT ages in the klippe. As the klippe was folded, flexural slip occurred producing localized shear zones.

This study was the first attempt to compare the geology of the Almora-Dadeldhura klippe across the India-Nepal border and compile the available dataset in order to obtain an unbiased interpretation of the kinematic history of the thrust belt. This study showed the scope of reinterpreting the same data set for supporting a model and how a pre-determined hypothesis can affect interpretation. Rather than proving or disproving a model, it is shown how the same data can be used to support different models. This emphasizes the necessity to generate more data from the Almora-Dadeldhura klippe.

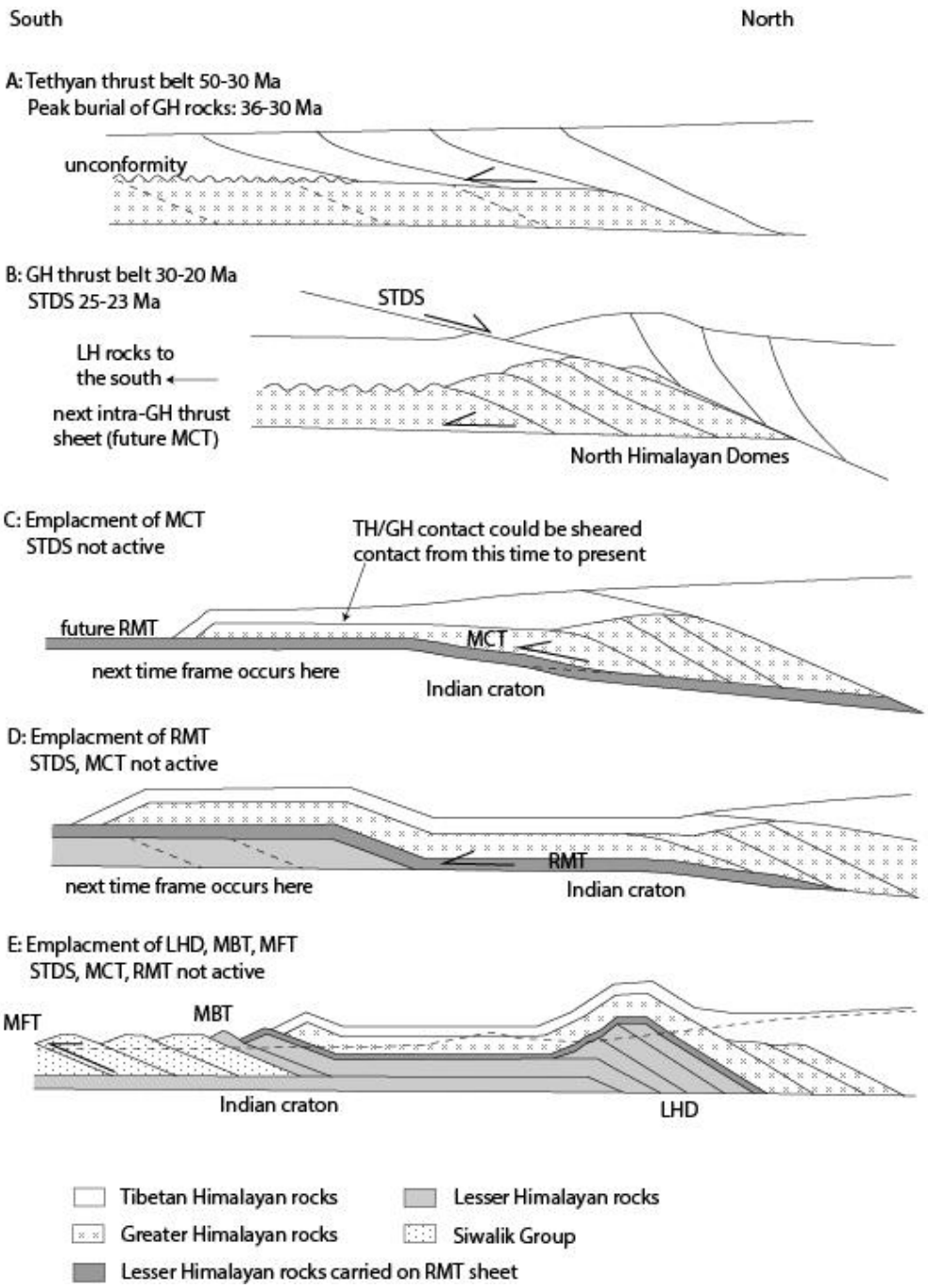

Figure 17. General kinematic evolution of the Himalayan thrust belt. Because of the variability of the timing of frames C, D, and E across different sections, an absolute time is not given above; however, it is discussed of the text. Dashed lines in C and D are future locations of faults. Dashed line in E is the current erosion level. Scale changes in every time frame. Abbreviations: TH: Tibetan Himalayan rocks; GH: Greater Himalayan rocks; LH: Lesser Himalayan rocks; STDS: South Tibetan Detachment System; MCT: Main Central thrust; RMT: Ramgarh-Munsiari thrust; LHD: Lesser Himalayan Duplex; MBT: Main Boundary thrust; MFT: Main Frontal thrust. Figure by Delores M. Robinson.

The sheared contact between the Tethyan and Greater Himalayan rocks in the Almora-Dadeldhura klippe has a different deformation history from the STDS in this region and can be reinterpreted as another intra-Greater Himalayan shear zone. The shear zones inside the klippe worked as a localized, out-of-sequence thrust in brittle regime as late as 7-5 Ma, when the deformation front was active further towards foreland, in the Main Boundary thrust (MBT). This observation supports the critical taper model, which predicts out-of-sequence, <5 km thrusting in the shear zone. Different timing of motion of the klippe shear zones and the STDS in this region thwarts the validation of the channel flow model. The premise of the wedge insertion model is the interpretation of a merging of the basal shear zone (MCT) in the klippe with the Tila shear zone. This interpretation is extrapolated from available structural data, which can be interpreted otherwise. As more metamorphic data becomes available from the klippe rocks, it can be used to put the critical taper model to further test. The metamorphic history can be used to correlate the same from the main outcrops of the Greater Himalayan and Tethyan Himalayan rocks, in order to have a robust stratigraphic correlation and understand if the burial timing and mechanism was similar towards the foreland in the klippe.

10. REFERENCES

Aitchison, J., 2010, Comparative anatomy of orogenic systems: Comparing the Himalaya-Tibet with New England. New England Orogen Conference NEO 2010, Australia: University of New England.

Antolín, B., Godin, L., Wemmer, K., and Nagy, C., 2013, Kinematics of the Dadeldhura klippe shear zones (W Nepal): implications for the foreland evolution of the Himalayan metamorphic core: Terra Nova, v. 25, no. 4, p. 282-291.

Beaumont, C., Jamieson, R. A., Nguyen, M. H., and Lee, B., 2001, Himalayan tectonics explained by extrusion of a low-viscosity crustal channel coupled to focused surface denudation: Nature, v. 414, no. 6865, p. 738-742.

Bera, M. K., Sarkar, A., Chakrabarty, P. P., Loyal, R., Sanyal, P., 2008, Marine to continental transition in Himalayan foreland, Bulletin Geological Society of America, v. 120, p. 1214-1232.

Brown, R.L., Gibson, H.D., 2006, An argument for channel flow in the southern Canadian Cordillera and comparison with Himalayan tectonics. In: Law, R., Searle, M.P., Godin, L. (Eds.), Channel Flow, Ductile Extrusion, and Exhumation in Continental Collision Zones. Geological Society of London Special Publication, v. 268, p. 543–559.

Burchfiel, B. C., and Royden, L. H., 1985, North-south extension within the convergent Himalayan region: Geology, v. 13, no. 10, p. 679-682.

Burchfiel, B. C., Zhiliang, C., Hodges, K. V., Yuping, L., Royden, L. H., Changrong, D., and Jiene, X., 1992, The South Tibetan Detachment System, Himalayan Orogen: Extension Contemporaneous with and Parallel to Shortening in a Collisional Mountain Belt: Geological Society of America Special Papers, v. 269, p. 1-41.

Burg, J. P., Brunel, M., Gapais, D., Chen, G. M., and Liu, G. H., 1984, Deformation of leucogranites of the crystalline Main Central Sheet in southern Tibet (China): Journal of Structural Geology, v. 6, no. 5, p. 535-542.

Carosi, R., Montomoli, C., Rubatto, D., Visonà, D., 2013, Leucogranite intruding the South Tibetan Detachment in western Nepal: implications for exhumation models in the Himalayas, Terra Nova, v. 25 (6), p. 478-489.

Célérier, J., Harrison, T.M., Webb, A.A.G., Yin, A., 2009, The Kumaun and Garwhal Lesser Himalaya, India; part 1, structure and stratigraphy. Geological Society of America Bulletin., v. 121, p. 1262–1280.

Copeland, P., Harrison, T. M., Kidd, W. S. F., Ronghua, X. & Yuquan, Z., 1987, Rapid early Miocene acceleration of uplift in the Gangdese belt, Xizang (southern Tibet), and its bearing on accomodation mecanisms of the Indian-Asia collision, Earth and Planetary Science Letters, v. 86, p. 240–252.

Dahlen, F.A., 1984, Non-cohesive critical Coulomb wedges—an exact solution: Journal of Geophysical Research, v. 89, p. 125–133

Dahlen, F.A., 1990, Critical taper model of fold-and-thrust belts and accretionary wedges: Annual Review of Earth and Planetary Sciences, v. 18, p. 55-99.

Davis, D., Suppe, J., and Dahlen, F.A., 1983, Mechanics of fold-and-thrust belts and accretionary wedges: Journal of Geophysical Research, v. 88 (B2), p. 1153-1178.

Decelles, P. G., Cavazza, W., 1999, A comparison of fluvial megafans in the Cordilleran (Upper Cretaceous) and modern Himalayan foreland basin systems, Bulletin of the Geological Society of America, v. 111, p. 1315-1334.

DeCelles, P. G., Gehrels, G. E., Quade, J., LaReau, B., and Spurlin, M., 2000, Tectonic implications of U-Pb zircon ages of the Himalayan orogenic belt in Nepal: Science, v. 288, no. 5465, p. 497-499.

DeCelles, P. G., Robinson, D. M., Quade, J., Ojha, T., Garzione, C. N., Copeland, P., and Upreti, B. N., 2001, Stratigraphy, structure, and tectonic evolution of the Himalayan fold-thrust belt in western Nepal: Tectonics, v. 20, no. 4, p. 487-509.

DeCelles, P.G., Gehrels, G.E., Quade, J., Ojha, T.P., Kapp, P.A., Upreti, B.N. , 1998, Neogene foreland basin deposits, erosional unroofing, and the kinematic history of the Himalayan fold-thrust belt, western Nepal: Geological Society of America Bulletin, v. 110, p. 2–21.

Frank, W., Fuchs, G., 1970, Geological investigations in western Nepal and their significance for the geology of the Himalayas: Geologischen Rundschau, v. 59, p. 552–580.

Fritz, H., Tenczer, V., Hauzenberger, C., Wallbrecher, E., Muhongo, S., 2009, Hot granulite nappes — tectonic styles and thermal evolution of the Proterozoic granulite belts in East Africa. Tectonophysics, v. 477, p. 160–173.

Gansser, A., 1964, The Geology of the Himalayas Wiley Interscience, New York, p. 289.

Garzanti, E., 1999, Stratigraphy and sedimentary history of the Nepal Tethys Himalaya passive margin, Journal of Asian Earth Sciences, v. 17 (5-6), p. 805-827.

Gehrels, G. E., DeCelles, P. G., Ojha, T. P., and Upreti, B. N., 2006, Geologic and U–Pb geochronologic evidence for early Paleozoic tectonism in the Dadeldhura thrust sheet, far-west Nepal Himalaya: Journal of Asian Earth Sciences, v. 28, no. 4–6, p. 385-408.

Godin, L., Grujic, D., Law, R., Searle, M.P., 2006, Crustal flow, extrusion, and exhumation in continental collision collision zones: an introduction. In: Law, R., Searle, M.P., Godin, L. (Eds.), Channel Flow, Ductile Extrusion, and Exhumation in Continental Collision Zones, Geological Society of London Special Publication, v. 268, p. 1–23.

Grujic, D., Casey, M., Davidson, C., Hollister, L. S., Kündig, R., Pavlis, T., and Schmid, S., 1996, Ductile extrusion of the Higher Himalayan Crystalline in Bhutan: evidence from quartz microfabrics: Tectonophysics, v. 260, no. 1, p. 21-43.

Hauck, M.L., Nelson, K.D., Brown, W., Zhao, W., and Ross, A.R., 1998, Crustal structure of the Himalayan orogen at ~90°E longitude from Project INDEPTH deep reflection profiles: Tectonics, v. 17, p. 481-500.

He, D., Webb, A. A. G., Larson, K. P., and Schmitt, A. K., 2016, Extrusion vs. duplexing models of Himalayan mountain building 2: The South Tibet detachment at the Dadeldhura klippe: Tectonophysics, v. 667, p. 87-107.

Heim, A., and Gansser, A., 1939, Central Himalaya: geological observations of the Swiss expedition 1936: Memoir of Swiss Society of Natural Science, v. 73, 245p.

Hodges, K. V., 2000, Tectonics of the Himalaya and southern Tibet from two perspectives, Geological Society of America Bulletin, v. 112 (3), p. 324-350.

Hodges, K.V., Walker, J.D., 1992, Extension in the Cretaceous Sevier orogen, North American Cordillera. Geological. Society of America Bulletin, v. 104, p. 560–569.

Hughes, N.C., Droser, M.L., 1992, Trace fossils from the Phe formation (Lower Cambrian), Zanskar Valley, northwestern India: Memoirs Queensland Museum, v. 32, p. 139–144.

Iaccarino, S., Montomoli, C., Carosi, R., Massonne, H. J., Visonà, D., 2017, Geology and tectono-metamorphic evolution of the Himalayan metamorphic core: Insights from the Mugu Karnali transect, Western Nepal (Central Himalaya), Journal of Metamorphic Geology, v. 35:3, pp. 301-325.

Jacobs, J., Thomas, R. J., 2004, Himalayan-type indenter-escape tectonics model for the southern part of the late Neoproterozoic-early Paleozoic East African-Antarctic orogen, Geology, v. 32, p. 721-724.

Jamieson, R.A., Beaumont, C., Nguyen, M.H., Culshaw, N.G., 2007, Syn-convergent ductile flow in variable-strength continental crust: numerical models with application to the western Grenville orogen. Tectonics, v. 26, TC5005.

Johnson, M. R. W., Oliver, G. J. H., Parrish, R. R., and Johnson, S. P., 2001, Synthrusting metamorphism, cooling, and erosion of the Himalayan Kathmandu Complex, Nepal: Tectonics, v. 20, no. 3, p. 394-415.

Joshi, M., 1999, Evolution of the basal shear zone of the Almora Klippe, Kumaun Himalaya,in: A.K. Jain, R.M. Manickvasagam (Eds.), Geodynamics of the NW Himalaya, Gondawana Research Group, v. 6, p. 69–80.

Joshi, M., and Tiwari, A. N., 2009, Structural events and metamorphic consequences in Almora Nappe, during Himalayan collision tectonics: Journal of Asian Earth Sciences, v. 34, no. 3, p. 326-335.

Kaphle, K. P., 1992, Geology, petrology, and geochemistry of the Dadeldhura granite massif, far western Nepal. Kashmir Journal of Geology, v. 10, p. 75-92.

Kohn, M. J., 2008, P-T-t data from central Nepal support critical taper and repudiate large-scale channel flow of the Greater Himalayan Sequence, Geological Society of America Bulletin, v. 120, p. 259-273.

Kohn, M.J., Paul, S.K., and Corrie, S.L., 2010, The lower Lesser Himalayan Sequence: A Paleoproterozoic arc on the northern margin of the Indian plate: Geological Society of America Bulletin, v. 122, p. 323–335.

Kuiper, Y.D., Williams, P.F., Kruse, S., 2006, Possibility of channel flow in the southern Canadian Cordillera: a new approach to explain existing data. In: Law, R., Searle, M.P., Godin, L. (Eds.), Channel Flow, Ductile Extrusion, and Exhumation in Continental Collision Zones. Geological Society London Special Publication, v. 268, p. 589–611.

Kutzbach, J. E. & Ziegler, A. M., 1993, Simulations of late Permian climate and biomes with an atmosphere-ocean model: comparisons with observations. Phil. Trans. R. Soc. Land. V. B 341, p. 327–340.

La Roche, R. S., Godin, L., Cottle, J. M., and Kellett, D. A., 2016, Direct shear fabric dating constrains early Oligocene onset of the South Tibetan detachment in the western Nepal Himalaya: Geology, v. 44, no. 6, p. 403-406.

Law, R. D., 2014, Deformation thermometry based on quartz c-axis fabrics and recrystallization microstructures: A review., Journal of Structural Geology, v. 66, p. 129-161.

LeFort., P, 1975, Himalayas: The collided range, present knowledge of the continental arc: American Journal of Science, v. 275(A), p. 1-44.

Long, S.P., Gordon, S.M., Young, J.P., and Soignard, E, 2016, Temperature and strain gradients through Lesser Himalayan rocks and across the Main Central thrust, south-central Bhutan: implications for transport-parallel stretching and inverted metamorphism: Tectonics, v. 35, p. 1863-1891.

Mandal, S., 2014, Structural, kinematic and geochronologic evolution of the the Himalayan fold-thrust belt in Kumaun, Uttaranchal, northwest India: Ph.D. thesis, 173 p., The University of Alabama, USA.

Mandal, S., D. M. Robinson, M. J. Kohn, S. Khanal, O. Das, and S. Bose, 2016, Zircon U-Pb ages and Hf isotopes of the Askot klippe, Kumaun, northwest India: Implications for Paleoproterozoic tectonics, basin evolution and associated metallogeny of the northern Indian cratonic margin, Tectonics, v. 35,

Martin, A. J., 2017, A review of Himalayan stratigraphy, magmatism, and structure, Gondwana Research, v. 49, p. 42-80.

McClelland, W.C., and Gilotti, J.A., 2003, Late-stage extensional exhumation of high-pressure granulites in the Greenland Caledonides. Geology, v. 31, p. 259–262.

Molnar, P., England, P. & Martinod, J., 1993, Mantle dynamics uplift of the Tibetan plateau, and the Indian monsoon. Rev. Geophys., v. 31, p. 357–396.

Molnar, P., England, P., 1990, Late Cenozoic uplift of mountain ranges and global climate change: Chicken or egg? Nature, v. 346, p. 29-34.

Montemagni, C., Iaccarino, S., Montomoli, C., Carosi, R., Jain, A. K., Villa I. M., Age constraints on the deformation style of the South Tibetan Detachment System in Garhwal Himalaya, Italian Journal of Geosciences, v. 137 (2), p. 1-14.

Montomoli, C., Iaccarino, S., Carosi, R., Langone, A., Visonà, D., 2013, Tectonometamorphic discontinuities within the Greater Himalayan Sequence in Western Nepal (Central Himalaya): insights on the exhumation of crystalline rocks, Tectonophysics, v. 608, p. 1349-1370.

Næraa, T., Konnerup-Madsen, J., Hageskov, B., and Paudel, L. P., 2007, Structure and petrology of the Dadeldhura Group, far western Nepal, Himalaya: Journal of Nepal Geological Survey, v. 35, p. 21-28.

Najman, Y., 2006, The detrital record of orogenesis: A review of approaches and techniques used in the Himalayan sedimentary basins: Earth-Science Reviews, v. 72, p. 1–72.

Nelson, K.D., and 27 others, 1996, Partially molten middle crust beneath southern Tibet: synthesis of project INDEPTH results: Science, v. 274, p. 1684-1695.

Ojha, T. P., Butler, R., Decelles, P., Quade, J., 2008, Magnetic polarity stratigraphy of the Neogene foreland basin deposits of Nepal, Basin Research, v. 21(1), p. 61 - 90

Parrish, R. R., Hodges, V., 1996, Isotopic constraints on the age and provenance of the Lesser and Greater Himalayan sequences, Nepalese Himalaya, Geological Society of America Bulletin, v. 108 (7), p. 904-911.

Patel, R. C., Singh, P., and Lal, N., 2015, Thrusting and back-thrusting as post-emplacement kinematics of the Almora klippe: Insights from Low-temperature thermochronology: Tectonophysics, v. 653, p. 41-51.

Powers, P. M., Lillie, R. J., and Yeats, R. S., 1998, Structure and shortening of the Kangra and Dehra Dun reentrants, Sub-Himalaya, India: Geological Society of America Bulletin, v. 110, no. 8, p. 1010-1027.

Raimondo, T., Collins, A.S., Hand, M., Walker-Hallam, A., Smithies, R.H., Evins, P.M., Howard, H.M., 2009, Ediacaran intracontinental channel flow, Geology, v. 37, p. 291–294.

Ramstein, G., Fluteau, F., Besse, J., Joussaume, S., 1997, Effect of orogeny, plate motion and land–sea distribution on Eurasian climate change over the past 30 million years, Nature, v. 386, p. 788–795.

Ratschbacher, L., Frisch, W., Liu, G., Chen, C., 1994, Distributed deformation in southern and western Tibet during and after the India–Asia collision. J. Geophys. Res., v. 99, p. 19817–19945.

Rawat, R., and Sharma, R., 2011, Features and characterization of graphite in Almora Crystallines and their implication for the graphite formation in Lesser Himalaya, India: Journal of Asian Earth Sciences, v. 42, no. 1–2, p. 51-64.

Rivers, T., 2008, Assembly and preservation of lower, mid, and upper orogenic crust in the Grenville Province — implications for the evolution of large hot long-duration orogens. Precambrian Research, v. 167, p. 237–259.

Robinson, D. M., DeCelles, P. G., and Copeland, P., 2006, Tectonic evolution of the Himalayan thrust belt in western Nepal: Implications for channel flow models: Geological Society of America Bulletin, v. 118, no. 7-8, p. 865-885.

Robinson, D. M., DeCelles, P. G., Patchett, P. J., Garzione C., 2001, The kinematic evolution of the Nepalese Himalaya interpreted from Nd isotopes, Earth and Planetary Science Letters, v. 192 (4), p. 507-521.

Robinson, D. M., McQuarrie, N., 2012, Pulsed deformation and variable slip rates within the central Himalayan thrust belt, Lithosphere, v. 4 (5), p. 449-464.

Robinson, D., Decelles, P. G., Garzione, C., Pearson, O., Harrison, T., and Catlos, E., 2003, Kinematic model for the Main Central thrust in Nepal: Geology, v. 31, no. 4, p. 359-362.

Robinson, D.M., and Pearson, O., 2013, Was Himalayan normal faulting triggered by initiation of the Ramgarh-Munsiari thrust and development of the Lesser Himalayan duplex: International Journal of Earth Sciences, v. 102, p. 1773-1790.

Robison, D. M., Martin, A. J., 2014, Reconstructing the Greater Indian margin: A balanced cross section in central Nepal focusing on the Lesser Himalayan duplex, Tectonics, v. 33 (11), p. 2143-2168.

Rösler,W., Metzler,W., Appel, E., 1997, Neogene magnetic polarity stratigraphy of some fluviatile Siwalik sections, Nepal, Geophysics J. Int., v. 130, p. 89-111.

Rupke, J., 1974, Stratigraphic and structural evolution of the Kumaun Lesser Himalaya: Sedimentary Geology, v. 11(2), p. 81-265.

Searle, M. P., Metcalfe, R. P., Rex, A. J., Norry, M. J., 1993, Field relations, petrogenesis and emplacement of the Bhagirathi leucogranite, Garhwal Himalaya, Geological Society, London, Special Publications, v. 74, p. 429-444.

Searle, M. P., Metcalfe, R. P., Rex, A. J., Norry, M. J., 1993, Field relations, petrogenesis and emplacement of the Bhagirathi leucogranite, Garhwal Himalaya, Geological Society, London, Special Publications, v. 74 (1), p. 429-444.

Searle, M. P., Noble, S. R., Hurford, A. J., Rex, D. C., 1999, Age of crustal melting, emplacement and exhumation history of the Shivling leucogranite, Garhwal Himalaya, Geological Magazine, v. 136 (5), p. 513-525.

Selleck, B.W., McLelland, J.M., Bickford, M.E., 2005, Granite emplacement during tectonic exhumation: the Adirondack example. Geology, v. 33, p. 781–784.

Sen, K., Chaudhury, R., Pfänder, J., 2015, 40Ar–39Ar age constraint on deformation and brittle–ductile transition of the Main Central Thrust and the South Tibetan Detachment zone from Dhauliganga valley, Garhwal …, Journal of Geodynamics, v. 88, p. 1-13.

Singh, P., Patel, R. C., 2017, Post-emplacement kinematics and exhumation history of the Almora klippe of the Kumaun–Garhwal Himalaya, NW India: revealed by fission track thermochronology, Int J Earth Sci (Geol Rundsch), v. 106, p. 2189.

Srivastava, P., and Mitra, G., 1994, Thrust geometries and deep structure of the outer and lesser Himalaya, Kumaon and Garhwal (India): Implications for evolution of the Himalayan fold-and-thrust belt: Tectonics, v. 13, no. 1, p. 89-109.

Srivastava, P., and Mitra, G., 1996, Deformation mechanisms and inverted thermal profile in the North Almora Thrust mylonite zone, Kumaon Lesser Himalaya, India: Journal of Structural Geology, v. 18, no. 1, p. 27-39.

Stöcklin, J., 1980, Geology of Nepal and its regional frame: Thirty-third William Smith Lecture, v. 137, no. 1, p. 1-34.

Thiede, R. C., Bookhagen, B., Arrowsmith, J. R., Sobel, E. R., and Strecker, M. R., 2004, Climatic control on rapid exhumation along the Southern Himalayan Front: Earth and Planetary Science Letters, v. 222, no. 3–4, p. 791-806.

Trivedi, J.R., Gopalan, K., Valdiya, K.S., 1984, Rb–Sr ages of granitic rocks within the Lesser Himalayan Nappes, Kumaun, India: Journal of the Geological Society of India, v. 25, p. 641–654.

Upreti, B. N., 1999, An overview of the stratigraphy and tectonics of the Nepal Himalaya: Journal of Asian Earth Sciences, v. 17, no. 5–6, p. 577-606.

Upreti, B. N., and Le Fort, P., 1999, Lesser Himalayan crystalline nappes of Nepal: Problems of their origin: Geological Society of America Special Papers, v. 328, p. 225-238.

Valdiya, K. S., 1980, Geology of kumaun lesser Himalaya, Wadia Institute of Himalayan Geology.

Valdiya, K. S., and Kotlia, B. S., 2001, Fluvial geomorphic evidence for Late Quaternary reactivation of a synclinally folded nappe in Kumaun Lesser Himalaya: Journal of the Geological Society of India, v. 58, no. 4, p. 303-317.

van der Beek, P., Litty, C., Baudin, M., Mercier, J., Robert, X., and Hardwick, E., 2016, Contrasting tectonically driven exhumation and incision patterns, western versus central Nepal Himalaya: Geology, v. 44, no. 4, p. 327-330.

Webb, A. A. G., Yin, A., Harrison, T. M., Célérier, J., Gehrels, G. E., Manning, C. E., and Grove, M., 2011, Cenozoic tectonic history of the Himachal Himalaya (northwestern India) and its constraints on the formation mechanism of the Himalayan orogen: Geosphere, v. 7, no. 4, p. 1013-1061.

Webb, A.A.G., Yin, A., Harrison, T.M., Célérier, J., Burgess, W.P., 2007, The leading edge of the Greater Himalayan Crystallines revealed in the NW Indian Himalaya: implications for the evolution of the Himalayan Orogen, Geology, v. 35, p. 955–958.

Weller, O.M., St-Onge, M.R., Searle, M.P., Waters, D.J., Rayner, N., Chung, S.L., Palin, R.M., and Chen, S., 2015, Quantifying the P–T–t conditions of north-south Lhasa terrane accretion: new insight into the pre-Himalayan architecture of the Tibetan plateau. Journal of Metamorphic Geology, v. 33, p. 91–113.

Wells, M.L., 1997, Alternating contraction and extension in the hinterlands of orogenic belts: an example from the Raft River Mountains, Utah Geological Society American Bulletin, v. 109, p. 107–126.

Wiesmayr, G., and Grasemann, B., 2002, Eohimalayan fold and thrust belt: Implications for the geodynamic evolution of the NW-Himalaya (India): Tectonics, v. 21, no. 6, p. 8-1-8-18.

Yakymchuk, C., Godin, L., 2012. Coupled role of deformation and metamorphism in the construction of inverted metamorphic sequences: an example from far-northwest Nepal, Journal of Metamorphic Geology, v. 30, p. 513–535.

Yin, A., 2002, Passive-roof thrust model for the emplacement of the Pelona-Orocopia Schist in southern California, United States: Geology, v. 30, no. 2, p. 183-186.

Yin, A., 2006, Cenozoic tectonic evolution of the Himalayan orogen as constrained by along-strike variation of structural geometry, exhumation history, and foreland sedimentation. Earth Science Reviews, v. 76, 1–131.

Zhao, W., Nelson, K. D., Che, J., Quo, J., Lu, D., Wu, C., and Liu, X., 1993, Deep seismic reflection evidence for continental underthrusting beneath southern Tibet: Nature, v. 366, no. 6455, p. 557-559.